Int. J. Anal. Appl. (2026), 24:137

International Journal of Analysis and Applications

Fractional-Order Modeling and PINN-Based Analysis of Monkeypox Transmission with Optimal Control

Shanmugam Manikandan[1], Prabakaran Raghavendran[2,3], Rithik Sam Abraham[4], Mana Donganont[5,*], Vediyappan Govindan[6]

[1]*Department of Mathematics, Vel Tech High Tech Dr.Rangarajan Dr.Sakunthala Engineering College, Avadi, Chennai, India*

[2]*Department of Mathematics, Easwari Engineering College, 18 Bharathi Salai, Ramapuram Chennai-600089, Tamil Nadu, India*

[3]*Department of Mathematics and Science Education, Faculty of Education, Harran University, Sanliurfa, Turkey*

[4]*Department of Biotechnology, Monash University, Melbourne, Australia*

[5]*School of Science, University of Phayao, Phayao 56000, Thailand*

[6]*Department of Mathematics, Hindustan Institute of Technology and Science, Chennai, Tamil Nadu, India*

[*]*Corresponding author:* mana.do@up.ac.th

Abstract. Monkeypox, a zoonotic viral disease, is becoming a major health issue worldwide and requires advanced mathematical models to understand its complicated transmission patterns. A new monkeypox transmission model based on Atangana-Baleanu-Caputo (ABC) fractional derivatives, which considers memory and hereditary effects due to the interactions of human and animal populations, is proposed in this study. Fixed-point theory is applied to prove the existence and uniqueness of solutions and also an optimal control problem is posed with the aim of reducing the number of infected people and at the same time lowering the costs of treatment and preventive measures required, the necessary optimality conditions are derived using Pontryagin's Maximum Principle. A Physics-Informed Neural Network (PINN) framework is used not only to approximate the solution of the ABC-fractional system but also to infer key model parameters directly from the governing dynamics in order to improve the applicability and computational efficiency of the model. Numerical experiments reveal a very close match between the solutions derived from the PINN approach and the results obtained from conventional fractional numerical methods, thus pointing to the considerable impact of fractional-order effects on the dynamics of the epidemic, notably in terms of delayed outbreak peaks and extended infection periods. The combined approach of fractional calculus and AI constitutes a powerful and versatile tool for outbreak prediction, thus facilitating the health authorities to make well-informed decisions.

Received: Mar. 9, 2026.

2020 *Mathematics Subject Classification.* 34A08, 34A12, 92D30, 68T07, 49K15.

Key words and phrases. monkeypox; ABC-fractional derivative; physics-informed neural networks; optimal control; epidemic modeling; fractional-order dynamics.

https://doi.org/10.28924/2291-8639-24-2026-137
ISSN: 2291-8639

1. Introduction

Beginning in 1958, the introduction of two monkeys from Singapore to Copenhagen sparked a smallpox-like outbreak among them. Subsequent similar outbreaks occurred among captive monkey populations in the USA throughout the following decade, yet human infections were not reported. It's noteworthy that the virus responsible for human monkeypox shares a genetic relation with the smallpox virus, both classified within the Poxviridae family and Orthopoxvirus genus [12].

The first reported case of human infection with monkeypox occurred in 1970, in the Democratic Republic of the Congo, where most reported cases continue to occur. At that time, however, most countries had already discontinued Vaccinia vaccine production due to the campaign to eliminate smallpox by 1980 [1, 8]. This meant that the levels of immunity against related viruses were lowered. Over time, however, despite the initial predominance in African nations, cases of monkeypox among people were described in different countries. Detection of cases in non-endemic regions in May 2022 prompted the World Health Organization to declare a global epidemic for the virus in July 2022.

Monkeypox may be transmitted through animal and human contacts or even within humans. Incubation is normally between 5 to 21 days, with the middle period standing at 6 to 13 days. Symptoms take a period of 2 to 4 weeks and then include rash, lymph node inflammation, and fever. However, when the case is more complex, there is the possibility of developing pneumonia, encephalitis, or even eye infections. The current observed rate of fatality associated with monkeypox has been between 3% and 6%, mainly because it is prevalent in the young population. However, one should note the possibility of those with HIV facing serious consequences due to the monkeypox virus infection [**?**].

There have been numerous models created to analyze infectious disease dynamics using mathematical techniques. The Susceptible-Infected-Recovered (SIR) model proposed by Kermack and McKendrick in 1927 is the backbone of mathematical studies on infectious diseases [10]. This model has been improved over time to account for the dynamical nature of the disease and the increasing specificity of the parameter values [13]. Moreover, there have been stability analyses of monkeypox disease models for both human and non-human primate interactions conducted by Usman and Adamu [19]. Moreover, there have been specific studies on the role of quarantine and awareness campaigns in monkeypox virus modeling studies [18]. Recently, there was the emergence of the Caputo-Fabrizio fractional model proposed by Peter et al. to analyze the monkeypox virus's potential exponential growth pattern [14]. Yet, the quest to find the optimal method to control monkeypox outbreaks is an area still being studied as it began with the evaluation by Bhunu et al. of using humans treated and recovered and rodents recovered as categories in models along with sensitivity analysis techniques to guide prevention and treatment methods [15, 17].

The aim of the paper is to propose a new theoretical framework for the dynamics of monkeypox virus transmission. The model differentiates between humans and rodents in the total population

as recognized natural hosts of the virus. Model parameter estimates are performed in a manner that considers transmission factors, both human-to-human and animal-to-human zoonotic pathways. The existence of the proposed symmetry model solutions is determined by fixed-point theory and iterative procedure. Further optimum condition was determined by the Pontryagin's maximum principle and showed the effectiveness of such strategy under numerical simulations [7]. Along with stability analyses, there were some epidemiological models that have examined optimum prevention and treatment strategies by ensuring minimum number of infections with maximum cost-effectiveness [4, 11]. A significant tool in this direction is the theory of optimal control [5, 16]. There exist plenty of works which look into the dynamics of various biological systems and their optimum control.

Monkeypox, which is becoming more prevalent globally, has made it clear that mathematical and computational modeling are essential tools to predict and hence understand the disease dynamics. The common practice of modeling infectious diseases using simple integer-order epidemic models has often overlooked the effects of time and heredity inherent in diseases like monkeypox that take some time to develop, and these diseases have a tendency to reoccur due to immunity that is not yet full-blown. Such effects are better captured by fractional-order modeling, particularly that involving the Anagnostopulos derivative. However, the application of these models is still limited as they require advanced mathematics and are also time-consuming especially when they have to be combined with multi-compartment systems and capture little or polluted data on the disease's epidemiology. The maternal-child approach, where Physics-Informed Neural Networks (PINNs) models, is close to the development of a patient-specific model that will have the dual benefits of being based on the mechanistic knowledge and being able to pick up on applied dynamics.

The originality of this research is the joint effort to apply the ABC-fractional modeling, the optimization of control theory, and the artificial intelligence learning in a single framework for the monkeypox spreading model. In contrast to the studies done in the past, the present research works on three main fronts at the same time: (i) memory and hereditary effects are being replicated in the system through a fractional-order model; (ii) the optimal control geometry is designed to minimize infections and control costs based on Pontryagin's Maximum Principle; and (iii) Physics-Informed Neural Networks are used to get the fractional system solution and the uncertain epidemiological parameters are inferred directly from the governing dynamics. This integrative method brings together smooth, uninterrupted, and computing-efficient solutions while at the same time giving public health decision-making the much-needed actionable insights, which is a capability that has not been explored much in the literature to date.

Along with the merits of the proposed framework, the drawbacks have to be acknowledged. The present model is based on the presumption of homogeneous mixing for all human and animal populations and ignores the effects of heterogeneity and randomness in space that could have a say on transmission in actual scenarios. Furthermore, the precision of parameter estimation in the

PINN framework is dependent on the availability and quality of epidemiological data. The requirement for computation increases with the complexity of the model in terms of dimensionality or with finer temporal resolution, although PINNs still do better than traditional fractional numerical solvers regarding this. One of the future extensions could be tackling these issues through the introduction of spatial-temporal dynamics, stochastic processes, and adaptive control strategies, which will greatly enhance predictive capability for a broader spectrum of infectious diseases.

2. Preliminaries

This section provides a brief definition, for the fractional order derivatives

Definition 2.1. The left Riemann-Liouville (RL) integral [2,9] is

$$({}_0I^{\alpha}x)(\varpi) = \frac{1}{\Gamma(\alpha)}\int_0^{\varpi}(\varpi - s)^{\alpha-1}x(s)ds, \tag{2.1}$$

where $\alpha > 0$.

Definition 2.2. The (AB)derivative in sense of Caputo [2,9] is

$$({}_0^{ABC}D^{\alpha}x)(\varpi) = \frac{B(\alpha)}{1-\alpha}\int_o^{\varpi}x'(s)\Big[-\alpha\frac{(\varpi - s)^{\alpha}}{1-\alpha}\Big]ds,$$

x′ ∈ H′ (a,b),$\alpha \in [0,1]$ and a≤b.

Definition 2.3. The fractional order integral [2,9] of 2.1 is

$$({}_0^{AB}I^{\alpha}x)(\varpi) = \frac{1-\alpha}{B(\alpha)}x(\varpi) + \frac{\alpha}{B(\alpha)}({}_0I^{\alpha}x)(\varpi) \tag{2.2}$$

where ${}_0I^{\alpha}$ denotes the left (RL) integral given in 2.1.

3. Model Formulation

The total population at time ϖ, denoted by $N_H(\varpi)$, is divided into the human $(N_H(\varpi))$ and animal $(N_A(\varpi))$ populations. The total human population is further sub-divided into the seven mutually- exclusive compartments of the susceptible $(S_H(\varpi))$, vaccinated $(V_H(\varpi))$, exposed $(E_H(\varpi))$, asymptomatic $(A_H(\varpi))$, symptomatic $(I_H(\varpi))$, isolated $(T_H(\varpi))$ and treated individuals who recover from monkeypox infection $(R_H(\varpi))$. Similarly, the total animal population is sub-divided into the susceptible $(S_A(\varpi))$, exposed $(E_A(\varpi))$, infected $(I_A(\varpi))$ and recovered $(R_A(\varpi))$ animal sub-population. Thus,

$$\begin{aligned}
\frac{dS_H(\varpi)}{d\varpi} &= \Lambda_h - \lambda_H S_H(\varpi) + \omega V_H(\varpi) - (v + \mu_h)S_H(\varpi),\\
\frac{dV_H(\varpi)}{d\varpi} &= vS_H(\varpi) - (\omega + \mu_h)V_H(\varpi),\\
\frac{dE_H(\varpi)}{d\varpi} &= \lambda_H S_H(\varpi) - (\theta\rho + \theta(1-\rho) + \mu_h)E_H(\varpi),\\
\frac{dA_H(\varpi)}{d\varpi} &= \theta\rho E_H(\varpi) - (\sigma + \phi + \mu_h)A_H(\varpi),
\end{aligned} \tag{3.1}$$

$$\begin{aligned}
\frac{dI_H(\varpi)}{d\varpi} &= \phi A_H(\varpi) + \theta(1-\rho)E_H(\varpi) - (\tau + \mu_h + \delta_h)I_H(\varpi),\\
\frac{dT_H(\varpi)}{d\varpi} &= \tau I_H(\varpi) - (\gamma_h + \mu_h + \delta_h)T_H(\varpi),\\
\frac{dR_H(\varpi)}{d\varpi} &= \sigma A_H(\varpi) + \gamma_h T_H(\varpi) - \mu_h R_H(\varpi),\\
\frac{dS_A(\varpi)}{d\varpi} &= \Lambda_a - \lambda_A S_A(\varpi) - \mu_a S_A(\varpi),\\
\frac{dE_A(\varpi)}{d\varpi} &= \lambda_A S_A(\varpi) - (\varphi + \mu_a)E_A(\varpi),\\
\frac{dI_A(\varpi)}{d\varpi} &= \varphi E_A(\varpi) - (\gamma_a + \mu_a + \delta_a)I_A(\varpi),\\
\frac{dR_A(\varpi)}{d\varpi} &= \gamma_a I_A(\varpi) - \mu_a R_A(\varpi).
\end{aligned}$$

The susceptible population (for both human and animals) are increased by the recruitment of new individuals (assumed susceptible) into the population at a rate $\Lambda_h(\Lambda_a)$ for human (animal). Susceptible individuals acquire monkeypox infection, following effective contact with infected animals and humans (i.e. those in the A_H, I_H and I_A classes, at a rate λ_H, given by

$$\lambda_H = \left(\frac{\beta_h(I_H+\eta A_H)}{N_H} + \frac{\beta_a I_A}{N_A}\right),$$

Similarly, the susceptible animals acquire the infection following effective contact with an infected animal (i.e., those in the I_A class) at a rate

$$\lambda_A = \frac{\beta_a I_A}{N_A},$$

Furthermore, η is the modification parameter associated with the reduced infectiousness of individuals in the asymptomatic class (A_H) . Individuals in E_H class progresses to the infected classes (A_H) and (I_H) at rate θ while ρ is the proportion of individuals that progressed to class (A_H) . Similarly, the animals in E_A progresses to the infected class I_A at a rate φ. Individuals in the asymptomatic class either recover naturally and move to the recovered class R_H at a rate σ or progress to the the symptomatic class at a rate ϕ. Also, individuals in I_H compartment who show symptoms of monkeypox virus are moved to the isolation centre (T_H) for treatment at a rate τ. The parameter γ_h accounts for the recovery rate of individuals in T_H after treatment, while γ_a is the recovery rate of the animals in I_A class. Furthermore, natural death rate $\mu_h(\mu_a)$ occurs in all the epidemiological classes of human (animal) population while individuals in I_H and T_H classes suffer an additional monkeypox induced death at rate δ_h .The animal population in I_A equally die due to monkeypox infection at a rate δ_a. Combining all these definitions and assumptions, it follows that the new monkeypox model is given by the system of differential equations, the variables of the model are tabulated in Table 1.The variables and parameters of the model are interpreted in Table 1. To introduce the ABC-fractional derivative model for monkeypox, we replace the first-order time derivative on the left side of Equation 3.1 with the ABC-fractional derivative as described in the equation. Here is a potential formulation of the updated ABC-fractional model for monkeypox.

$$
\begin{aligned}
{}_0^{ABC}D_\omega^\alpha(S_H(\omega)) &= \Lambda_h - \lambda_H S_H(\omega) + \omega V_H(\omega) - (\upsilon + \mu_h)S_H(\omega),\\
{}_0^{ABC}D_\omega^\alpha(V_H(\omega)) &= \upsilon S_H(\omega) - (\omega + \mu_h)V_H(\omega),\\
{}_0^{ABC}D_\omega^\alpha(E_H(\omega)) &= \lambda_H S_H(\omega) - (\theta\rho + \theta(1-\rho) + \mu_h)E_H(\omega),\\
{}_0^{ABC}D_\omega^\alpha(A_H(\omega)) &= \theta\rho E_H(\omega) - (\sigma + \phi + \mu_h)A_H(\omega),\\
{}_0^{ABC}D_\omega^\alpha(I_H(\omega)) &= \phi A_H(\omega) + \theta(1-\rho)E_H(\omega) - (\tau + \mu_h + \delta_h)I_H(\omega),\\
{}_0^{ABC}D_\omega^\alpha(T_H(\omega)) &= \tau I_H(\omega) - (\gamma_h + \mu_h + \delta_h)T_H(\omega),\\
{}_0^{ABC}D_\omega^\alpha(R_H(\omega)) &= \sigma A_H(\omega) + \gamma_h T_H(\omega) - \mu_h R_H(\omega),\\
{}_0^{ABC}D_\omega^\alpha(S_A(\omega)) &= \Lambda_a - \lambda_A S_A(\omega) - \mu_a S_A(\omega),\\
{}_0^{ABC}D_\omega^\alpha(E_A(\omega)) &= \lambda_A S_A(\omega) - (\varphi + \mu_a)E_A(\omega),\\
{}_0^{ABC}D_\omega^\alpha(I_A(\omega)) &= \varphi E_A(\omega) - (\gamma_a + \mu_a + \delta_a)I_A(\omega),\\
{}_0^{ABC}D_\omega^\alpha(R_A(\omega)) &= \gamma_a I_A(\omega) - \mu_a R_A(\omega).
\end{aligned}
\tag{3.2}
$$

where the initial condition are
$S_H(0) = S_{H_0}$,$V_H(0) = V_{H_0}$,$E_H(0) = E_{H_0}$,$A_H(0) = A_{H_0}$,$I_H(0) = I_{H_0}$,$T_H(0) = T_{H_0}$,
$R_H(0) = R_{H_0}$,$S_A(0) = S_{A_0}$,$E_A(0) = E_{A_0}$,$I_A(0) = I_{A_0}$,and $R_A(0) = R_{A_0}$, and the definitions of parameters in the model are listed in Table 1.

Table 1. Description of parameters in the monkeypox model

Variables	Parameters Interpretation	Value	Ref
Λ_h	Recruitment rate into S_H	0.029	[3]
υ	Effective vaccination rate	0.85	[20]
μ_h	Natural death rate for humans	0.02	(Assumed)
δ_h	Death rate due to monkeypox virus	0.1	(Fitted)
θ	Rate of progression from E_H to A_H	0.20	(Assumed)
ρ	Proportion of exposed moving to A_H	0.6	(Assumed)
ϕ	Progression from A_H to I_H	0.3	(Assumed)
σ	Natural recovery rate of asymptomatics	0.4	(Fitted)
τ	Treatment rate for symptomatics	0.6	(Assumed)
ω	Waning rate of monkeypox vaccine	0.60	(Assumed)
η	Modification parameter for reduced transmission	0.6	(Fitted)
β_h	Probability of human-to-human transmission	0.000063	[3]
β_a	Probability of animal-to-human transmission	0.000252	[3]
Λ_a	Recruitment rate into animal population	0.02	(Assumed)
μ_a	Natural death rate for animals	0.2	[7]
φ	Rate of progression in animals	0.3	[19]
δ_a	Death rate due to monkeypox in animals	0.4	[3]

4. Existence of Solution

This section presents the findings from the existence result for the ABC-fractional order monkeypox transmission model using fixed point

Definition 4.1. Let ϕ is a given function depending on the time and $\alpha \in (0, 1)$, then, the α-order AB integral is characterized as

$$ {}_0^{AB}I_{\omega}^{\alpha}\phi(\omega) = \aleph_1(\alpha)\phi(\omega) + \aleph_2(\alpha)\int_0^{\omega}(\omega-\vartheta)^{\alpha-1}\phi(\vartheta)d\vartheta, \tag{4.1}$$

where $\aleph_1(\alpha)=\frac{1-\alpha}{B(\alpha)}$ and $\aleph_2(\alpha)=\frac{\alpha}{B(\alpha)\Gamma_{\alpha}}$.

suppose F(γ) be a Banach space of all continuous function on γ=[0,b] and Q=F(γ)×F(γ)×F(γ)×F(γ)×F(γ)×F(γ)×F(γ) ×F(γ) ×F(γ) ×F(γ) with the norm $\|(S_H, V_H, E_H, A_H, I_H, T_H, R_H, S_A, E_A, I_A, R_A)\| = \|S_H\| + \|V_H\| + \|E_H\| + \|A_H\| + \|I_H\| + \|T_H\| + \|R_H\| + \|S_A\| + \|E_A\| + \|I_A\| + \|R_A\|$. where

$$\begin{aligned}
&\|S_H\| = \sup\{|S_H(\omega)| : \omega \in \gamma\}, \|V_H\| = \sup\{|V_H(\omega)| : \omega \in \gamma\},\\
&\|E_H\| = \sup\{|E_H(\omega)| : \omega \in \gamma\}, \|A_H\| = \sup\{|A_H(\omega)| : \omega \in \gamma\},\\
&\|I_H\| = \sup\{|I_H(\omega)| : \omega \in \gamma\}, \ \|T_H\| = \sup\{|T_H(\omega)| : \omega \in \gamma\},\\
&\|R_H\| = \sup\{|R_H(\omega)| : \omega \in \gamma\}, \|S_A\| = \sup\{|S_a(\omega)| : \omega \in \gamma\},\\
&\|E_A\| = \sup\{|E_A(\omega)| : \omega \in \gamma\}, \ \|I_A\| = \sup\{|I_A(\omega)| : \omega \in \gamma\},\\
&\|R_A\| = \sup\{|R_A(\omega)| : \omega \in \gamma\}.
\end{aligned}$$

Making use of the fractional integral operator as shown in an essential not to be both side 2.2, we obtain

$$\begin{aligned}
S_H(\omega) - S_H(0) &= {}_0^{AB}I_{\omega}^{\alpha}[\Lambda_h - \lambda_H S_H(\omega) + \omega V_H(\omega) - (v+\mu_h)S_H(\omega)],\\
V_H(\omega) - V_H(0) &= {}_0^{AB}I_{\omega}^{\alpha}[vS_H(\omega) - (\omega+\mu_h)V_H(\omega)],\\
E_h(\omega) - E_H(0) &= {}_0^{AB}I_{\omega}^{\alpha}[\lambda_H S_H(\omega) - (\theta\rho + \theta(1-\rho) + \mu_h)E_H(\omega)],\\
A_H(\omega) - A_H(0) &= {}_0^{AB}I_{\omega}^{\alpha}[\theta\rho E_H(\omega) - (\sigma+\phi+\mu_h)A_H(\omega)],\\
I_H(\omega) - I_H(0) &= {}_0^{AB}I_{\omega}^{\alpha}[\phi A_H(\omega) + \theta(1-\rho)E_H(\omega) - (\tau+\mu_h+\delta_h)I_H(\omega)],\\
T_H(\omega) - T_H(0) &= {}_0^{AB}I_{\omega}^{\alpha}[\tau I_H(\omega) - (\gamma_h+\mu_h+\delta_h)T_H(\omega)],\\
R_H(\omega) - R_H(0) &= {}_0^{AB}I_{\omega}^{\alpha}[\sigma A_H(\omega) + \gamma_h T_H(\omega) - \mu_h R_H(\omega)],\\
S_A(\omega) - S_A(0) &= {}_0^{AB}I_{\omega}^{\alpha}[\Lambda_a - \lambda_A S_A(\omega) - \mu_a S_A(\omega)],\\
E_A(\omega) - E_A(0) &= {}_0^{AB}I_{\omega}^{\alpha}[\lambda_A S_A(\omega) - (\varphi+\mu_a)E_A(\omega)],\\
I_A(\omega) - I_A(0) &= {}_0^{AB}I_{\omega}^{\alpha}[\varphi E_A(\omega) - (\gamma_a+\mu_a+\delta_a)I_A(\omega)],\\
R_A(\omega) - R_A(0) &= {}_0^{AB}I_{\omega}^{\alpha}[\gamma_a I_A(\omega) - \mu_a R_A(\omega)].
\end{aligned} \tag{4.2}$$

By using 4.1 in 4.2, we get

$$\begin{aligned}
S_H(\varpi) - S_H(0) &= \aleph_1(\alpha)K_1(\varpi, S_H(\varpi)) + \aleph_2(\alpha)_0I^\alpha K_1(\varpi, S_H(\varpi)),\\
V_H(\varpi) - V_H(0) &= \aleph_1(\alpha)K_2(\varpi, V_H(\varpi)) + \aleph_2(\alpha)_0I^\alpha K_2(\varpi, V_H(\varpi)),\\
E_H(\varpi) - E_H(0) &= \aleph_1(\alpha)K_3(\varpi, E_H(\varpi)) + \aleph_2(\alpha)_0I^\alpha K_3(\varpi, E_H(\varpi)),\\
A_H(\varpi) - A_H(0) &= \aleph_1(\alpha)K_4(\varpi, A_H(\varpi)) + \aleph_2(\alpha)_0I^\alpha K_4(\varpi, A_H(\varpi)),\\
I_H(\varpi) - I_H(0) &= \aleph_1(\alpha)K_5(\varpi, I_H(\varpi)) + \aleph_2(\alpha)_0I^\alpha K_5(\varpi, I_H(\varpi)),\\
T_H(\varpi) - T_H(0) &= \aleph_1(\alpha)K_6(\varpi, T_H(\varpi)) + \aleph_2(\alpha)_0I^\alpha K_6(\varpi, T_H(\varpi)),\\
R_H(\varpi) - R_H(0) &= \aleph_1(\alpha)K_7(\varpi, R_H(\varpi)) + \aleph_2(\alpha)_0I^\alpha K_7(\varpi, R_H(\varpi)),\\
S_A(\varpi) - S_A(0) &= \aleph_1(\alpha)K_8(\varpi, S_A(\varpi)) + \aleph_2(\alpha)_0I^\alpha K_8(\varpi, S_A(\varpi)),\\
E_A(\varpi) - E_A(0) &= \aleph_1(\alpha)K_9(\varpi, E_A(\varpi)) + \aleph_2(\alpha)_0I^\alpha K_9(\varpi, E_A(\varpi)),\\
I_A(\varpi) - I_A(0) &= \aleph_1(\alpha)K_{10}(\varpi, I_A(\varpi)) + \aleph_2(\alpha)_0I^\alpha K_{10}(\varpi, I_A(\varpi)),\\
R_A(\varpi) - R_A(0) &= \aleph_1(\alpha)K_{11}(\varpi, R_A(\varpi)) + \aleph_2(\alpha)_0I^\alpha K_{11}(\varpi, R_A(\varpi)).
\end{aligned} \tag{4.3}$$

where

$$\begin{aligned}
K_1(\varpi, S_H(\varpi)) &= \Lambda_h - \lambda_H S_H(\varpi) + \omega V_H(\varpi) - (v + \mu_h)S_H(\varpi),\\
K_2(\varpi, V_H(\varpi)) &= vS_H(\varpi) - (\omega + \mu_h)V_H(\varpi),\\
K_3(\varpi, E_H(\varpi)) &= \lambda_H S_H(\varpi) - (\theta\rho + \theta(1-\rho) + \mu_h)E_H(\varpi),\\
K_4(\varpi, A_H(\varpi)) &= \theta\rho E_H(\varpi) - (\sigma + \phi + \mu_h)A_H(\varpi),\\
K_5(\varpi, I_H(\varpi)) &= \phi A_H(\varpi) + \theta(1-\rho)E_H(\varpi) - (\tau + \mu_h + \delta_h)I_H(\varpi),\\
K_6(\varpi, T_H(\varpi)) &= \tau I_H(\varpi) - (\gamma_h + \mu_h + \delta_h)T_H(\varpi),\\
K_7(\varpi, R_H(\varpi)) &= \sigma A_H(\varpi) + \gamma_h T_H(\varpi) - \mu_h R_H(\varpi),\\
K_8(\varpi, S_A(\varpi)) &= \Lambda_a - \lambda_A S_A(\varpi) - \mu_a S_A(\varpi),\\
K_9(\varpi, E_A(\varpi)) &= \lambda_A S_A(\varpi) - (\varphi + \mu_a)E_A(\varpi),\\
K_{10}(\varpi, I_A(\varpi)) &= \varphi E_A(\varpi) - (\gamma_a + \mu_a + \delta_a)I_A(\varpi),\\
K_{11}(\varpi, R_A(\varpi)) &= \gamma_a I_A(\varpi) - \mu_a R_A(\varpi).
\end{aligned} \tag{4.4}$$

The expression $K_1, K_2, K_3, K_4, K_5, K_6, K_7, K_8, K_9, K_{10}$ and K_{11} are holds the lipschitz criterion iff $S_H, V_H, E_H, A_H,$
$I_H, T_H, R_H, S_A, E_A, I_A$, and R_A has an upper bound.

If we assume that there are two functions, $S_H(\varpi)$ and $S_H * (\varpi)$, we have

$$\begin{aligned}
\|K_1(\varpi, S_H(\varpi)) - K_1(\varpi, S_H^*(\varpi))\| &= \|\Lambda_h - \lambda_H(S_H(\varpi) - S_H^*(\varpi))\\
&\quad + \omega V_H(S_H(\varpi) - S_H^*(\varpi))\|\\
&\leq \| - \lambda_H - (v + \mu_h)(S_H(\varpi) - S_H^*(\varpi))\|\\
&\leq (\lambda_H + (v + \mu_h))\|S_H(\varpi) - S_H^*(\varpi)\|
\end{aligned} \tag{4.5}$$

Considering $\eta_1 =(\lambda_H + (v + \mu_h))\|S_H(\varpi) - S_H^*(\varpi)\|$ and λ_H is a bounded function, then we get

$$\|K_1(\varpi, S_H(\varpi)) - K_1(\varpi, S_H^*(\varpi))\| \leq \eta_1\|S_H(\varpi) - S_H^*(\varpi)\|, \tag{4.6}$$

With the similar procedure, the result deduced to

$$\begin{aligned}
\|K_2(\varpi, V_H(\varpi)) - K_2(\varpi, V_H^*(\varpi))\| &\leq \eta_2\|V_H(\varpi) - V_H^*(\varpi)\|,\\
\|K_3(\varpi, E_H(\varpi)) - K_3(\varpi, E_H^*(\varpi))\| &\leq \eta_3\|E_H(\varpi) - E_H^*(\varpi)\|,\\
\|K_4(\varpi, A_H(\varpi)) - K_4(\varpi, A_H^*(\varpi))\| &\leq \eta_4\|A_H(\varpi) - A_H^*(\varpi)\|,\\
\|K_5(\varpi, I_H(\varpi)) - K_5(\varpi, I_H^*(\varpi))\| &\leq \eta_5\|I_H(\varpi) - I_H^*(\varpi)\|,\\
\|K_6(\varpi, T_H(\varpi)) - K_6(\varpi, T_H^*(\varpi))\| &\leq \eta_6\|T_H(\varpi) - T_H^*(\varpi)\|,\\
\|K_7(\varpi, R_H(\varpi)) - K_7(\varpi, R_H^*(\varpi))\| &\leq \eta_7\|R_H(\varpi) - R_H^*(\varpi)\|,\\
\|K_8(\varpi, S_A(\varpi)) - K_8(\varpi, S_A^*(\varpi))\| &\leq \eta_8\|S_A(\varpi) - S_A^*(\varpi)\|,\\
\|K_9(\varpi, E_A(\varpi)) - K_9(\varpi, E_A^*(\varpi))\| &\leq \eta_9\|E_A(\varpi) - E_A^*(\varpi)\|,\\
\|K_{10}(\varpi, I_A(\varpi)) - K_{10}(\varpi, I_A^*(\varpi))\| &\leq \eta_{10}\|I_A(\varpi) - I_A^*(\varpi)\|,\\
\|K_{11}(\varpi, R_A(\varpi)) - K_{11}(\varpi, R_A^*(\varpi))\| &\leq \eta_{11}\|R_A(\varpi) - R_A^*(\varpi)\|.
\end{aligned} \tag{4.7}$$

Hence, all the seven function $K_1, K_2, K_3, K_4, K_5, K_6, K_7, K_8, K_9, K_{10}$, and K_{11} holds the Lipschitz criterion. Recurively, the expression in 4.3 writing it as

$$\begin{aligned}
S_{H_n}(\varpi) =&\aleph_1(\alpha)K_1(\varpi, S_{H_{,n-1}}(\varpi)) + \aleph_2(\alpha){}_0I^\alpha K_1(\varpi, S_{H_{,n-1}}(\varpi)),\\
V_{H_n}(\varpi) =&\aleph_1(\alpha)K_2(\varpi, V_{H_{,n-1}}(\varpi)) + \aleph_2(\alpha){}_0I^\alpha K_2(\varpi, V_{H_{,n-1}}(\varpi)),\\
E_{H_n}(\varpi) =&\aleph_1(\alpha)K_3(\varpi, E_{H_{,n-1}}(\varpi)) + \aleph_2(\alpha){}_0I^\alpha K_3(\varpi, E_{H_{,n-1}}(\varpi)),\\
A_{H_n}(\varpi) =&\aleph_1(\alpha)K_4(\varpi, A_{H_{,n-1}}(\varpi)) + \aleph_2(\alpha){}_0I^\alpha K_4(\varpi, A_{H_{,n-1}}(\varpi)),\\
I_{H_n}(\varpi) =&\aleph_1(\alpha)K_5(\varpi, I_{H_{,n-1}}(\varpi)) + \aleph_2(\alpha){}_0I^\alpha K_5(\varpi, I_{H_{,n-1}}(\varpi)),\\
T_{H_n}(\varpi) =&\aleph_1(\alpha)K_6(\varpi, T_{H_{,n-1}}(\varpi)) + \aleph_2(\alpha){}_0I^\alpha K_6(\varpi, T_{H_{,n-1}}(\varpi)),\\
R_{H_n}(\varpi) =&\aleph_1(\alpha)K_7(\varpi, R_{H_{,n-1}}(\varpi)) + \aleph_2(\alpha){}_0I^\alpha K_7(\varpi, R_{H_{,n-1}}(\varpi)),\\
S_{A_n}(\varpi) =&\aleph_1(\alpha)K_8(\varpi, S_{A_{,n-1}}(\varpi)) + \aleph_2(\alpha){}_0I^\alpha K_8(\varpi, S_{A_{,n-1}}(\varpi)),\\
E_{A_n}(\varpi) =&\aleph_1(\alpha)K_9(\varpi, E_{A_{,n-1}}(\varpi)) + \aleph_2(\alpha){}_0I^\alpha K_9(\varpi, E_{A_{,n-1}}(\varpi)),\\
I_{A_n}(\varpi) =&\aleph_1(\alpha)K_{10}(\varpi, I_{A_{,n-1}}(\varpi)) + \aleph_2(\alpha){}_0I^\alpha K_{10}(\varpi, I_{A_{,n-1}}(\varpi)),\\
R_{A_n}(\varpi) =&\aleph_1(\alpha)K_{11}(\varpi, R_{A_{,n-1}}(\varpi)) + \aleph_2(\alpha){}_0I^\alpha K_{11}(\varpi, R_{A_{,n-1}}(\varpi)).
\end{aligned} \tag{4.8}$$

along with the inital starting point $S_{H_0}(\varpi) = S_H(0)$, $V_{H_0}(\varpi) = V_H(0)$, $E_{H_0}(\varpi) = E_H(0)$, $A_{H_0}(\varpi) = A_H(0)$, $I_{H_0}(\varpi) = I_H(0)$, $T_{H_0}(\varpi) = T_H(0)$, $R_{H_0}(\varpi) = R_H(0)$, $S_{A_0}(\varpi) = S_A(0)$, $E_{A_0}(\varpi) = E_A(0)$, $I_{A_0}(\varpi) = I_A(0)$, and $R_{A_0}(\varpi) = R_A(0)$.

By computing the difference between the succeeding terms, the following was determined.

$$
\begin{aligned}
\psi S_{H_{,n}}(\varpi) &= S_{H_n}(\varpi) - S_{H_{n-1}}(\varpi) \\
&= \aleph_1(\alpha)[K_1(\varpi, S_{H_{n-1}}(\varpi)) - K_1(\varpi, S_{H_{n-2}}(\varpi))] \\
&+ \aleph_2\ {}_0I^{\alpha}\ [K_1(\varpi, S_{H_{n-1}}(\varpi)) - K_1(\varpi, S_{H_{n-2}}(\varpi))], \\
\psi V_{H_{,n}}(\varpi) &= V_{H_n}(\varpi) - V_{H_{n-1}}(\varpi) \\
&= \aleph_1(\alpha)[K_2(\varpi, V_{H_{n-1}}(\varpi)) - K_2(\varpi, V_{H_{n-2}}(\varpi))] \\
&+ \aleph_2\ {}_0I^{\alpha}\ [K_2(\varpi, V_{H_{n-1}}(\varpi)) - K_2(\varpi, V_{H_{n-2}}(\varpi))], \\
\psi E_{H_{,n}}(\varpi) &= E_{H_n}(\varpi) - E_{H_{n-1}}(\varpi) \\
&= \aleph_1(\alpha)[K_3(\varpi, E_{H_{n-1}}(\varpi)) - K_3(\varpi, E_{H_{n-2}}(\varpi))] \\
&+ \aleph_2\ {}_0I^{\alpha}\ [K_E(\varpi, E_{H_{n-1}}(\varpi)) - K_3(\varpi, E_{H_{n-2}}(\varpi))], \\
\psi A_{H_{,n}}(\varpi) &= A_{H_n}(\varpi) - A_{H_{n-1}}(\varpi) \\
&= \aleph_1(\alpha)[K_4(\varpi, A_{H_{n-1}}(\varpi)) - K_4(\varpi, A_{H_{n-2}}(\varpi))] \\
&+ \aleph_2\ {}_0I^{\alpha}\ [K_4(\varpi, A_{H_{n-1}}(\varpi)) - K_4(\varpi, A_{H_{n-2}}(\varpi))], \\
\psi I_{H_{,n}}(\varpi) &= I_{H_n}(\varpi) - I_{H_{n-1}}(\varpi) \\
&= \aleph_1(\alpha)[K_5(\varpi, I_{H_{n-1}}(\varpi)) - K_5(\varpi, I_{H_{n-2}}(\varpi))] \\
&+ \aleph_2\ {}_0I^{\alpha}\ [K_5(\varpi, I_{H_{n-1}}(\varpi)) - K_5(\varpi, I_{H_{n-2}}(\varpi))], \\
\psi T_{H_{,n}}(\varpi) &= T_{H_n}(\varpi) - T_{H_{n-1}}(\varpi) \\
&= \aleph_1(\alpha)[K_6(\varpi, T_{H_{n-1}}(\varpi)) - K_6(\varpi, T_{H_{n-2}}(\varpi))] \\
&+ \aleph_2\ {}_0I^{\alpha}\ [K_6(\varpi, T_{H_{n-1}}(\varpi)) - K_6(\varpi, T_{H_{n-2}}(\varpi))], \\
\psi R_{H_{,n}}(\varpi) &= R_{H_n}(\varpi) - R_{H_{n-1}}(\varpi) \\
&= \aleph_1(\alpha)[K_7(\varpi, R_{H_{n-1}}(\varpi)) - K_7(\varpi, R_{H_{n-2}}(\varpi))] \\
&+ \aleph_2\ {}_0I^{\alpha}\ [K_7(\varpi, R_{H_{n-1}}(\varpi)) - K_7(\varpi, R_{H_{n-2}}(\varpi))], \\
\psi S_{A_{,n}}(\varpi) &= S_{A_n}(\varpi) - S_{A_{n-1}}(\varpi) \\
&= \aleph_1(\alpha)[K_8(\varpi, S_{A_{n-1}}(\varpi)) - K_8(\varpi, S_{A_{n-2}}(\varpi))] \\
&+ \aleph_2\ {}_0I^{\alpha}\ [K_8(\varpi, S_{A_{n-1}}(\varpi)) - K_8(\varpi, S_{A_{n-2}}(\varpi))], \\
\psi E_{A_{,n}}(\varpi) &= E_{A_n}(\varpi) - E_{A_{n-1}}(\varpi) \\
&= \aleph_1(\alpha)[K_9(\varpi, E_{A_{n-1}}(\varpi)) - K_9(\varpi, E_{A_{n-2}}(\varpi))] \\
&+ \aleph_2\ {}_0I^{\alpha}\ [K_9(\varpi, E_{A_{n-1}}(\varpi)) - K_9(\varpi, E_{A_{n-2}}(\varpi))], \\
\psi I_{A_{,n}}(\varpi) &= I_{A_n}(\varpi) - I_{A_{n-1}}(\varpi) \\
&= \aleph_1(\alpha)[K_{10}(\varpi, I_{A_{n-1}}(\varpi)) - K_{10}(\varpi, I_{A_{n-2}}(\varpi))] \\
&+ \aleph_2\ {}_0I^{\alpha}\ [K_{10}(\varpi, I_{A_{n-1}}(\varpi)) - K_{10}(\varpi, I_{A_{n-2}}(\varpi))], \\
\psi R_{A_{,n}}(\varpi) &= R_{A_n}(\varpi) - R_{A_{n-1}}(\varpi) \\
&= \aleph_1(\alpha)[K_{11}(\varpi, R_{A_{n-1}}(\varpi)) - K_{11}(\varpi, R_{A_{n-2}}(\varpi))] \\
&+ \aleph_2\ {}_0I^{\alpha}\ [K_{11}(\varpi, R_{A_{n-1}}(\varpi)) - K_{11}(\varpi, R_{A_{n-2}}(\varpi))].
\end{aligned}
\tag{4.9}
$$

It is critical to note that

$$S_{H_n}(\varpi) = \sum_{i=0}^{n} \psi S_{H,i}(\varpi), V_{H_n}(\varpi) = \sum_{i=0}^{n} \psi V_{H,i}(\varpi),$$
$$E_{H_n}(\varpi) = \sum_{i=0}^{n} \psi E_{H,i}(\varpi), A_{H_n}(\varpi) = \sum_{i=0}^{n} \psi A_{H,i}(\varpi),$$
$$I_{H_n}(\varpi) = \sum_{i=0}^{n} \psi I_{H,i}(\varpi), T_{H_n}(\varpi) = \sum_{i=0}^{n} \psi T_{H,i}(\varpi),$$

$$R_{H_n}(\varpi) = \sum_{i=0}^{n} \psi R_{H,i}(\varpi), S_{A_n}(\varpi) = \sum_{i=0}^{n} \psi S_{A,i}(\varpi),$$
$$E_{A_n}(\varpi) = \sum_{i=0}^{n} \psi E_{A,i}(\varpi), I_{A_n}(\varpi) = \sum_{i=0}^{n} \psi I_{A,i}(\varpi),$$
$$R_{A_n}(\varpi) = \sum_{i=0}^{n} \psi R_{A,i}(\varpi).$$

Additionally, utilising 4.8 and considering that

$$\psi S_{H,n}(\varpi) = S_{H_{n-1}}(\varpi) - S_{H_{n-2}}(\varpi),$$
$$\psi V_{H,n}(\varpi) = V_{H_{n-1}}(\varpi) - V_{H_{n-2}}(\varpi),$$
$$\psi E_{H,n}(\varpi) = E_{H_{n-1}}(\varpi) - E_{H_{n-2}}(\varpi),$$
$$\psi A_{H,n}(\varpi) = A_{H_{n-1}}(\varpi) - A_{H_{n-2}}(\varpi),$$
$$\psi I_{H,n}(\varpi) = I_{H_{n-1}}(\varpi) - I_{H_{n-2}}(\varpi),$$
$$\psi T_{H,n}(\varpi) = T_{H_{n-1}}(\varpi) - T_{H_{n-2}}(\varpi),$$
$$\psi R_{H,n}(\varpi) = R_{H_{n-1}}(\varpi) - R_{H_{n-2}}(\varpi),$$
$$\psi S_{A,n}(\varpi) = S_{A_{n-1}}(\varpi) - S_{A_{n-2}}(\varpi),$$
$$\psi E_{A,n}(\varpi) = E_{A_{n-1}}(\varpi) - E_{A_{n-2}}(\varpi),$$
$$\psi I_{A,n}(\varpi) = I_{A_{n-1}}(\varpi) - I_{A_{n-2}}(\varpi),$$
$$\psi R_{A,n}(\varpi) = R_{A_{n-1}}(\varpi) - R_{A_{n-2}}(\varpi),$$

we derive

$$\begin{aligned}
\|\psi S_{H,n}(\varpi)\| &= \aleph_1(\alpha)\eta_1\|\psi S_{H,n-1}(\varpi)\| + \aleph_2(\alpha)\eta_1\ {}_0I^{\alpha}\ \|\psi S_{H,n-1}(\varpi)\|,\\
\|\psi V_{H,n}(\varpi)\| &= \aleph_1(\alpha)\eta_2\|\psi V_{H,n-1}(\varpi)\| + \aleph_2(\alpha)\eta_2\ {}_0I^{\alpha}\ \|\psi V_{H,n-1}(\varpi)\|,\\
\|\psi E_{H,n}(\varpi)\| &= \aleph_1(\alpha)\eta_3\|\psi E_{H,n-1}(\varpi)\| + \aleph_2(\alpha)\eta_3\ {}_0I^{\alpha}\ \|\psi E_{H,n-1}(\varpi)\|,\\
\|\psi A_{H,n}(\varpi)\| &= \aleph_1(\alpha)\eta_4\|\psi A_{H,n-1}(\varpi)\| + \aleph_2(\alpha)\eta_4\ {}_0I^{\alpha}\ \|\psi A_{H,n-1}(\varpi)\|,\\
\|\psi I_{H,n}(\varpi)\| &= \aleph_1(\alpha)\eta_5\|\psi I_{H,n-1}(\varpi)\| + \aleph_2(\alpha)\eta_5\ {}_0I^{\alpha}\ \|\psi I_{H,n-1}(\varpi)\|,
\end{aligned} \tag{4.10}$$

$$\|\psi T_{H,n}(\varpi)\| = \aleph_1(\alpha)\eta_6\|\psi T_{H,n-1}(\varpi)\| + \aleph_2(\alpha)\eta_6\ {}_0I^{\alpha}\ \|\psi T_{H,n-1}(\varpi)\|,$$
$$\|\psi R_{H,n}(\varpi)\| = \aleph_1(\alpha)\eta_7\|\psi R_{H,n-1}(\varpi)\| + \aleph_2(\alpha)\eta_7\ {}_0I^{\alpha}\ \|\psi R_{H,n-1}(\varpi)\|,$$
$$\|\psi S_{A,n}(\varpi)\| = \aleph_1(\alpha)\eta_8\|\psi S_{A,n-1}(\varpi)\| + \aleph_2(\alpha)\eta_8\ {}_0I^{\alpha}\ \|\psi S_{A,n-1}(\varpi)\|,$$
$$\|\psi E_{A,n}(\varpi)\| = \aleph_1(\alpha)\eta_9\|\psi E_{A,n-1}(\varpi)\| + \aleph_2(\alpha)\eta_9\ {}_0I^{\alpha}\ \|\psi E_{A,n-1}(\varpi)\|,$$
$$\|\psi I_{A,n}(\varpi)\| = \aleph_1(\alpha)\eta_{10}\|\psi I_{A,n-1}(\varpi)\| + \aleph_2(\alpha)\eta_{10}\ {}_0I^{\alpha}\ \|\psi I_{A,n-1}(\varpi)\|,$$
$$\|\psi R_{A,n}(\varpi)\| = \aleph_1(\alpha)\eta_{11}\|\psi\psi R_{A,n-1}(\varpi)\| + \aleph_2(\alpha)\eta_{11}\ {}_0I^{\alpha}\ \|\psi R_{A,n-1}(\varpi)\|.$$

Theorem 4.1. Let the following condition satisfy.

$$\aleph_1(\alpha)\eta_i + \frac{\aleph_2(\alpha)}{\alpha}(\varpi)^{\alpha}\eta_i \leq 1, i = 1, 2, ..., 11 \tag{4.11}$$

Therefore, ϖ *in* [0,1] provides a unique solution for the fractional epidemic model 3.2.

Proof It is cleared that the function $S_H(\varpi), V_H(\varpi), E_H(\varpi), A_H(\varpi), I_H(\varpi), T_H(\varpi), R_H(\varpi)$, $S_A(\varpi), E_A(\varpi), I_A(\varpi)$, and $R_A(\varpi)$ are bounded. The expressions $K_1, K_2, K_3, K_4, K_5, K_6, K_7$, K_8, K_9, K_{10} and K_{11} holds the Lipschitz criterion. Therefore, using 4.10 and a recursive principle, the following concluded.

$$\|\psi S_{H,n}(\varpi)\| \leq \|S_{H_0}(\varpi)\left(\aleph_1(\alpha)\eta_1 + \frac{\aleph_2(\alpha)}{\alpha}(\varpi)^{\alpha}\eta_1\right)^n,$$
$$\|\psi V_{H,n}(\varpi)\| \leq \|V_{H_0}(\varpi)\left(\aleph_1(\alpha)\eta_2 + \frac{\aleph_2(\alpha)}{\alpha}(\varpi)^{\alpha}\eta_2\right)^n,$$
$$\|\psi E_{H,n}(\varpi)\| \leq \|E_{H_0}(\varpi)\left(\aleph_1(\alpha)\eta_3 + \frac{\aleph_2(\alpha)}{\alpha}(\varpi)^{\alpha}\eta_3\right)^n,$$
$$\|\psi A_{H,n}(\varpi)\| \leq \|A_{H_0}(\varpi)\left(\aleph_1(\alpha)\eta_4 + \frac{\aleph_2(\alpha)}{\alpha}(\varpi)^{\alpha}\eta_4\right)^n,$$
$$\|\psi I_{H,n}(\varpi)\| \leq \|I_{H_0}(\varpi)\left(\aleph_1(\alpha)\eta_5 + \frac{\aleph_2(\alpha)}{\alpha}(\varpi)^{\alpha}\eta_5\right)^n,$$
$$\|\psi T_{H,n}(\varpi)\| \leq \|T_{H_0}(\varpi)\left(\aleph_1(\alpha)\eta_6 + \frac{\aleph_2(\alpha)}{\alpha}(\varpi)^{\alpha}\eta_6\right)^n, \tag{4.12}$$
$$\|\psi R_{H,n}(\varpi)\| \leq \|R_{H_0}(\varpi)\left(\aleph_1(\alpha)\eta_7 + \frac{\aleph_2(\alpha)}{\alpha}(\varpi)^{\alpha}\eta_7\right)^n,$$
$$\|\psi S_{A,n}(\varpi)\| \leq \|S_{A_0}(\varpi)\left(\aleph_1(\alpha)\eta_8 + \frac{\aleph_2(\alpha)}{\alpha}(\varpi)^{\alpha}\eta_8\right)^n,$$
$$\|\psi E_{A,n}(\varpi)\| \leq \|E_{A_0}(\varpi)\left(\aleph_1(\alpha)\eta_9 + \frac{\aleph_2(\alpha)}{\alpha}(\varpi)^{\alpha}\eta_9\right)^n,$$
$$\|\psi I_{A,n}(\varpi)\| \leq \|I_{A_0}(\varpi)\left(\aleph_1(\alpha)\eta_{10} + \frac{\aleph_2(\alpha)}{\alpha}(\varpi)^{\alpha}\eta_{10}\right)^n,$$
$$\|\psi R_{A,n}(\varpi)\| \leq \|R_{A_0}(\varpi)\left(\aleph_1(\alpha)\eta_{11} + \frac{\aleph_2(\alpha)}{\alpha}(\varpi)^{\alpha}\eta_{11}\right)^n.$$

Therefore, it implies for n$\to\infty$, all mapping exists and fulfill
$\|\psi S_{H_{,n}}(\varpi)\| \to 0, \|\psi V_{H_{,n}}(\varpi)\| \to 0, \|\psi E_{H_{,n}}(\varpi)\| \to 0, \|\psi A_{H_{,n}}(\varpi)\| \to 0,$
$\|\psi I_{H_{,n}}(\varpi)\| \to 0, \|\psi T_{H_{,n}}(\varpi)\| \to 0, \|\psi R_{H_{,n}}(\varpi)\| \to 0, \|\psi S_{A_{,n}}(\varpi)\| \to 0,$
$\|\psi E_{A_{,n}}(\varpi)\| \to 0, \|\psi I_{A_{,n}}(\varpi)\| \to 0, \|\psi R_{A_{,n}}(\varpi)\| \to 0.$

Now, using the triangle inequality of 4.8, we obtain for every k

$$
\begin{aligned}
\|S_{H_{n+k}}(\varpi) - S_{H_n}(\varpi)\| &\leq \sum_{j=n+1}^{n+k} r_1^j = \frac{r_1^{n+1} - r_1^{n+k+1}}{1-r_1},\\
\|V_{H_{n+k}}(\varpi) - V_{H_n}(\varpi)\| &\leq \sum_{j=n+1}^{n+k} r_2^j = \frac{r_2^{n+1} - r_2^{n+k+1}}{1-r_2},\\
\|E_{H_{n+k}}(\varpi) - E_{H_n}(\varpi)\| &\leq \sum_{j=n+1}^{n+k} r_3^j = \frac{r_3^{n+1} - r_3^{n+k+1}}{1-r_3},\\
\|A_{H_{n+k}}(\varpi) - A_{H_n}(\varpi)\| &\leq \sum_{j=n+1}^{n+k} r_4^j = \frac{r_4^{n+1} - r_4^{n+k+1}}{1-r_4},\\
\|I_{H_{n+k}}(\varpi) - I_{H_n}(\varpi)\| &\leq \sum_{j=n+1}^{n+k} r_5^j = \frac{r_5^{n+1} - r_2^{n+k+1}}{1-r_5},\\
\|T_{H_{n+k}}(\varpi) - T_{H_n}(\varpi)\| &\leq \sum_{j=n+1}^{n+k} r_6^j = \frac{r_6^{n+1} - r_6^{n+k+1}}{1-r_6},\\
\|R_{H_{n+k}}(\varpi) - R_{H_n}(\varpi)\| &\leq \sum_{j=n+1}^{n+k} r_7^j = \frac{r_7^{n+1} - r_7^{n+k+1}}{1-r_7},\\
\|S_{A_{n+k}}(\varpi) - S_{A_n}(\varpi)\| &\leq \sum_{j=n+1}^{n+k} r_8^j = \frac{r_8^{n+1} - r_8^{n+k+1}}{1-r_8},\\
\|E_{A_{n+k}}(\varpi) - A_{A_n}(\varpi)\| &\leq \sum_{j=n+1}^{n+k} r_9^j = \frac{r_9^{n+1} - r_9^{n+k+1}}{1-r_9},\\
\|I_{A_{n+k}}(\varpi) - I_{A_n}(\varpi)\| &\leq \sum_{j=n+1}^{n+k} r_{10}^j = \frac{r_{10}^{n+1} - r_{10}^{n+k+1}}{1-r_{10}},\\
\|R_{A_{n+k}}(\varpi) - R_{A_n}(\varpi)\| &\leq \sum_{j=n+1}^{n+k} r_{11}^j = \frac{r_{11}^{n+1} - r_{11}^{n+k+1}}{1-r_{11}}.
\end{aligned}
\tag{4.13}
$$

where$r_i = \aleph_1(\alpha)\eta_i + \frac{\aleph_2(\alpha)}{\alpha}(\varpi)^\alpha \eta_i \leq 1$ by assumption, it follows that $S_H(\varpi), V_H(\varpi), E_H(\varpi), A_H(\varpi), I_H(\varpi), T_H(\varpi), R_H(\varpi), S_A(\varpi), E_A(\varpi), I_A(\varpi)$, and $R_A(\varpi)$ are Cauchy sequences and uniformly convergent in the Banach spaces $C(\gamma)$. As discussed in [9], employing the concept of limits in Eq. 4.8 as $n \to \infty$ demonstrates that the limit of these sequences provides a unique solution to the

fractional differential equation (FDE) 3.2. This confirms the existence of a solution that satisfies all conditions 4.11.

5. Optimal Control Analysis

We apply optimal control theory to the Monkeypox virus model outlined in Equation 3.2. To effectively mitigate the spread of the virus within the community, we consider four distinct control measures: Firstly, the Prevention/Isolation Control (u_1) aims to minimize contact between healthy and infected individuals. The measures encompassed in this control include encouraging behaviors like frequent handwashing, using sanitizers and masks, not attending meetings, and limited movements in regions where the number of cases is large. The second, which is Vaccination Control (u_2), is the vaccination of all people to minimize the further spread of the virus. It is proved that vaccination can reduce the level of infection and is necessary to reduce the risk of being infected. Moreover, the Rapid Testing Control (u_3) is aimed at the timely testing of people at the exposed phase to determine asymptomatic and symptomatic individuals. When it is detected, the infected people should be isolated or shut down in their houses to control additional spread. Finally, the Treatment Control Treatment Control is the topic of the treatment of people who have been infected by the Monkey pox virus but have not yet received any treatment. Be it asymptomatic or symptomatic, these people need to be treated and isolated in hospitals, quarantine centers or their homes. Parameters b_1 and b_2 are the rate of treating the asymptomatic and symptomatic, respectively, and b_3 is the rate of treating identified people.

$$\begin{aligned} J(u_1,u_2,u_3,u_4) =& min \int_0^T \Big[K_1E_H + K_2A_H + K_3I_H \\ &+ \frac{1}{2}(A_1u_1^2(\omega) + A_2u_2^2(\omega) + A_3u_3^2(\omega) + A_4u_4^2(\omega))\Big]dt. \end{aligned} \tag{5.1}$$

Model 3.2 is changed to model 5.1, subject to the state system, through incorporating the control variable.

$$\begin{aligned}
{}_0^{ABC}D_\omega^\alpha(S_H(\omega)) &= \Lambda_h - (1-u_1)\lambda_H S_H + \omega V_H - (vu_2+\mu_h)S_H,\\
{}_0^{ABC}D_\omega^\alpha(V_H(\omega)) &= vu_2S_H - (\omega+\mu_h)V_H,\\
{}_0^{ABC}D_\omega^\alpha(E_H(\omega)) &= \lambda_H S_H(1-u_1) - ((u_3)\theta\rho + \theta(1-\rho)+\mu_h)E_H,\\
{}_0^{ABC}D_\omega^\alpha(A_H(\omega)) &= \theta\rho u_3E_H - (\sigma+\phi+\mu_h+k_1u_4)A_H,\\
{}_0^{ABC}D_\omega^\alpha(I_H(\omega)) &= \phi k_1u_4A_H + \theta(1-\rho)u_3E_H - (\tau+\mu_h+\delta_h+k_2u_4)I_H,\\
{}_0^{ABC}D_\omega^\alpha(T_H(\omega)) &= \tau k_2u_4I_H - (\gamma_h+\mu_h+\delta_h+k_3u_4)T_H,\\
{}_0^{ABC}D_\omega^\alpha(R_H(\omega)) &= \sigma A_H + \gamma_hT_H - \mu_hR_H,\\
{}_0^{ABC}D_\omega^\alpha(S_A(\omega)) &= \Lambda_a - \lambda_AS_A - \mu_aS_A,\\
{}_0^{ABC}D_\omega^\alpha(E_A(\omega)) &= \lambda_AS_A - (\varphi+\mu_a)E_A,\\
{}_0^{ABC}D_\omega^\alpha(I_A(\omega)) &= \varphi E_A - (\gamma_a+\mu_a+\delta_a)I_A,\\
{}_0^{ABC}D_\omega^\alpha(R_A(\omega)) &= \gamma_aI_A - \mu_aR_A.
\end{aligned} \tag{5.2}$$

The control measures in equation 5.1 include Isolation (u_1), Vaccination (u_2), Rapid Testing (u_3), and Treatment (u_4). Rapid Testing is aimed at the timely detection of cases among exposed people, whereas Treatment is directed to giving them relevant care Our task is to find the controlling role that will maximize this goal.

$$J(u_1^*, u_2^*, u_3^*, u_4^*) = min\{J(u_1, u_2, u_3, u_4), u_1, u_2, u_3, u_4 \in U\} \tag{5.3}$$

In terms of the system 5.2, the control set is described as

$$U = \{(u_1, u_2, u_3, u_4)/u_i(\omega)\ 0 \leq u_i(\omega) \leq 1, i = 1, 2, 3, 4\}. \tag{5.4}$$

Applying Pontryagin's maximum principle reveals the conditions that an optimal solution must meet. This principle transforms equations 5.1–5.2 into a problem where the Hamiltonian H is minimized with respect to the control variables:

$$\begin{aligned}
H =& K_1E_H + K_2A_H + K_3I_H + \frac{1}{2}[(A_1u_1^2(\omega) + A_2u_2^2(\omega) \\
&+ A_3u_3^2(\omega) + A_4u_4^2(\omega))] \\
&+ \lambda_1(\omega)[\Lambda_h - (1-u_1)\lambda_H S_H + \omega V_H - (vu_2 + \mu_h)S_H], \\
&+ \lambda_2(\omega)[vu_2S_H - (\omega + \mu_h)V_H], \\
&+ \lambda_3(\omega)[\lambda_H S_H(1-u_1) - ((u_3)\theta\rho + \theta(1-\rho) + \mu_h)E_H], \\
&+ \lambda_4(\omega)[\theta\rho u_3E_H - (\sigma + \phi + \mu_h + k_1u_4)A_H], \\
&+ \lambda_5(\omega)[\phi k_1u_4A_H + \theta(1-\rho)u_3E_H - (\tau + \mu_h + \delta_h + k_2u_4)I_H], \\
&+ \lambda_6(\omega)[\tau k_2u_4I_H - (\gamma_h + \mu_h + \delta_h + k_3u_4)T_H], \\
&+ \lambda_7(\omega)[\sigma A_H + \gamma_h T_H - \mu_h R_H], \\
&+ \lambda_8(\omega)[\Lambda_a - \lambda_A S_A - \mu_a S_A], \\
&+ \lambda_9(\omega)[\lambda_A S_A - (\varphi + \mu_a)E_A], \\
&+ \lambda_{10}(\omega)[\varphi E_A - (\gamma_a + \mu_a + \delta_a)I_A], \\
&+ \lambda_{11}(\omega)[\gamma_a I_A - \mu_a R_A].
\end{aligned} \tag{5.5}$$

Where $\lambda_1(\omega), \lambda_2(\omega), \lambda_3, \lambda_4(\omega), \lambda_5(\omega), \lambda_6(\omega), \lambda_7(\omega), \lambda_8(\omega), \lambda_9(\omega), \lambda_{10}(\omega)$ and $\lambda_{11}(\omega)$ are made up of the adjoint variables. By analyzing the partial derivatives of Hamilton's equation (5.22) with respect to the corresponding state variable, we derive the solution for the system.
For the system of equations (5.18)–(5.19), we obtain the necessary optimality condition.:

$$\begin{aligned}
{}^{ABC}D_{0,\omega}^{\alpha}[S_H(\omega)] &= \frac{\partial \mathfrak{H}}{\partial \lambda_{S_H}}(\omega),\ {}^{ABC}D_{0,\omega}^{\alpha}[V_H(\omega)] = \frac{\partial \mathfrak{H}}{\partial \lambda_{V_H}}(\omega), \\
{}^{ABC}D_{0,\omega}^{\alpha}[E_H(\omega)] &= \frac{\partial \mathfrak{H}}{\partial \lambda_{E_H}}(\omega),\ {}^{ABC}D_{0,\omega}^{\alpha}[A_H(\omega)] = \frac{\partial \mathfrak{H}}{\partial \lambda_{A_H}}(\omega),
\end{aligned} \tag{5.6}$$

$$
\begin{aligned}
&{}^{ABC}D^{\alpha}_{0,\omega}[I_H(\omega)] = \frac{\partial \mathfrak{H}}{\partial \lambda_{I_H}}(\omega),\ {}^{ABC}D^{\alpha}_{0,\omega}[T_H(\omega)] = \frac{\partial \mathfrak{H}}{\partial \lambda_{T_H}}(\omega),\\
&{}^{ABC}D^{\alpha}_{0,\omega}[R_H(\omega)] = \frac{\partial \mathfrak{H}}{\partial \lambda_{R_H}}(\omega),\ {}^{ABC}D^{\alpha}_{0,\omega}[S_A(\omega)] = \frac{\partial \mathfrak{H}}{\partial \lambda_{S_A}}(\omega),\\
&{}^{ABC}D^{\alpha}_{0,\omega}[E_A(\omega)] = \frac{\partial \mathfrak{H}}{\partial \lambda_{E_A}}(\omega),\ {}^{ABC}D^{\alpha}_{0,\omega}[I_A(\omega)] = \frac{\partial \mathfrak{H}}{\partial \lambda_{I_A}}(\omega),\\
&{}^{ABC}D^{\alpha}_{0,\omega}[R_A(\omega)] = \frac{\partial \mathfrak{H}}{\partial \lambda_{R_A}}(\omega).\\
&{}^{ABC}_{\omega}D^{\alpha}_{T}[\lambda_{S_H}(\omega)] = -\frac{\partial \mathfrak{H}}{\partial S_H}(\omega),\ {}^{ABC}_{\omega}D^{\alpha}_{T}[\lambda_{V_H}(\omega)] = -\frac{\partial \mathfrak{H}}{\partial V_H}(\omega),\\
&{}^{ABC}_{\omega}D^{\alpha}_{T}[\lambda_{E_H}(\omega)] = -\frac{\partial \mathfrak{H}}{\partial E_H}(\omega),\ {}^{ABC}_{\omega}D^{\alpha}_{T}[\lambda_{A_H}(\omega)] = -\frac{\partial \mathfrak{H}}{\partial A_H}(\omega),\\
&{}^{ABC}_{\omega}D^{\alpha}_{T}[\lambda_{I_H}(\omega)] = -\frac{\partial \mathfrak{H}}{\partial I_H}(\omega),\ {}^{ABC}_{\omega}D^{\alpha}_{T}[\lambda_{T_H}(\omega)] = -\frac{\partial \mathfrak{H}}{\partial T_H}(\omega),\\
&{}^{ABC}_{\omega}D^{\alpha}_{T}[\lambda_{R_H}(\omega)] = -\frac{\partial \mathfrak{H}}{\partial R_H}(\omega),\ {}^{ABC}_{\omega}D^{\alpha}_{T}[\lambda_{S_A}(\omega)] = -\frac{\partial \mathfrak{H}}{\partial S_A}(\omega),\\
&{}^{ABC}_{\omega}D^{\alpha}_{T}[\lambda_{E_A}(\omega)] = -\frac{\partial \mathfrak{H}}{\partial E_A}(\omega),\ {}^{ABC}_{\omega}D^{\alpha}_{T}[\lambda_{I_A}(\omega)] = -\frac{\partial \mathfrak{H}}{\partial I_A}(\omega),\\
&{}^{ABC}_{\omega}D^{\alpha}_{T}[\lambda_{R_A}(\omega)] = -\frac{\partial \mathfrak{H}}{\partial R_A}(\omega),\ \frac{\partial \mathfrak{H}}{\partial u}(\omega) = 0.
\end{aligned}
\tag{5.7}
$$

Theorem 5.1. The above control system's solution (5.18) is $(u_{1*}, u_{2*}, u_{3*}, u_{4*})$ in view of the optimal controls., then we can find the adjoint variable $\lambda_i(\omega)$ for i=$S_H, V_H, E_H, A_H, I_H, T_H, R_H, S_A, E_A, I_A, R_A$ satisfying

$$
{}^{ABC}_{\omega}D^{\alpha}_{T}\lambda_i(\omega) = \frac{\partial \mathfrak{H}}{\partial i} \tag{5.8}
$$

where $i = i = S_H, V_H, E_H, A_H, I_H, T_H, R_H, S_A, E_A, I_A, R_A$ and with the transversality condition

$$
\lambda_i(T) = 0 \ for\ i = S_H, V_H, E_H, A_H, I_H, T_H, R_H, S_A, E_A, I_A, R_A. \tag{5.9}
$$

Furthermore, the optimal control variable $u_1^*, u_2^*, u_3^*, u_4^*$ are defined by

$$
\begin{aligned}
u_1^* &= min\left\{1, max\left[0, \frac{\lambda_H(\lambda_3 - \lambda_1)}{A_1}\right]\right\}\\
u_2^* &= min\left\{1, max\left[0, \frac{(\lambda_1 - \lambda_2)vS_H}{A_2}\right]\right\}\\
u_3^* &= min\left\{1, max\left[0, \frac{\theta E_H(\lambda_5 - \lambda_4)\varrho - \lambda_3 - \lambda_5}{A_3}\right]\right\}\\
u_4^* &= min\left\{1, max\left[0, \frac{\lambda_4\, k_1\, A_H + \lambda_5\, k_2\, I_H + \lambda_6\, k_3\, T_H}{A_4}\right]\right\}
\end{aligned}
\tag{5.10}
$$

Proof Using 5.9, we reach the adjoint system

$$\begin{aligned}
{}^{ABC}_{\omega}D^{\alpha}_{T}\lambda_{S_H}(\omega) =&(\lambda_1-\lambda_3)(1-u_1)(\lambda_H S_H)+(\lambda_1-\lambda_2)V\,u_2 S_H+\lambda_1\mu_h\\
{}^{ABC}_{\omega}D^{\alpha}_{T}\lambda_{V_H}(\omega) =&(\lambda_2-\lambda_1)u_2 S_H-(\omega+\mu_h)\lambda_2\\
{}^{ABC}_{\omega}D^{\alpha}_{T}\lambda_{E_H}(\omega) =&(\lambda_3-\lambda_1)(1-u_1)\lambda_H S_H+\lambda_3((1-u_3)\theta\rho+\mu_h)\\
&-\lambda_4\theta\rho u_3-\lambda_5(1-\rho)\theta u_3+K_1\\
{}^{ABC}_{\omega}D^{\alpha}_{T}\lambda_{A_H}(\omega) =&(\lambda_3-\lambda_4)u_3 E_H-(\sigma+\Phi+\mu_h+k_1u_1)+K_2\\
{}^{ABC}_{\omega}D^{\alpha}_{T}\lambda_{I_H}(\omega) =&\lambda_4\varphi+u_3\theta(1-\rho)\lambda_3-\lambda_5(\tau+\mu_h+\delta_h+k_2u_4)+K_3\\
{}^{ABC}_{\omega}D^{\alpha}_{T}\lambda_{T_H}(\omega) =&(\lambda_5-\lambda_6)k_2u_4\tau-(\gamma_h+\mu_h+\delta_h+k_3u_4)\\
{}^{ABC}_{\omega}D^{\alpha}_{T}\lambda_{R_H}(\omega) =&\sigma\lambda_4+\lambda_6\gamma_h-\mu_h\lambda_7\\
{}^{ABC}_{\omega}D^{\alpha}_{T}\lambda_{S_A}(\omega) =&(\lambda_8-\lambda_9)\lambda_A S_A-\mu_a\\
{}^{ABC}_{\omega}D^{\alpha}_{T}\lambda_{E_A}(\omega) =&\lambda_A S_A\lambda_8-(\varphi+\mu_a)\lambda_9\\
{}^{ABC}_{\omega}D^{\alpha}_{T}\lambda_{I_A}(\omega) =&(\lambda_9-\lambda_{10})\varphi-(\gamma_a+\mu_a+\delta_a)\\
{}^{ABC}_{\omega}D^{\alpha}_{T}\lambda_{R_A}(\omega) =&\lambda_{11}\mu_a
\end{aligned} \tag{5.11}$$

Also, by applying $\frac{\partial H}{\partial ui}=0$, we obtain (5.10) for i=1, 2, 3, 4.

6. Numerical Results for Optimal Control and Discussion

In this section, we numerically solve the optimal system described by Equation 3.2 using FDE 12 in MATLAB (online). The simulations are carried out for different values of the fractional order $\alpha \in (0,1]$, which enables the investigation of memory and hereditary effects in both human and animal populations. The numerical results clearly demonstrate how control interventions and fractional dynamics jointly shape the temporal evolution of the epidemic.

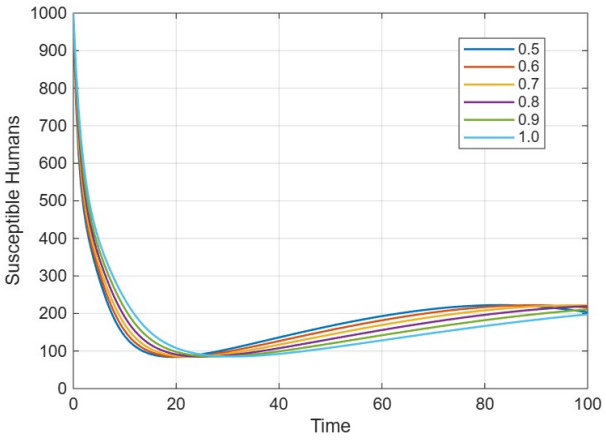

Figure 1. Susceptible Humans Individuals.

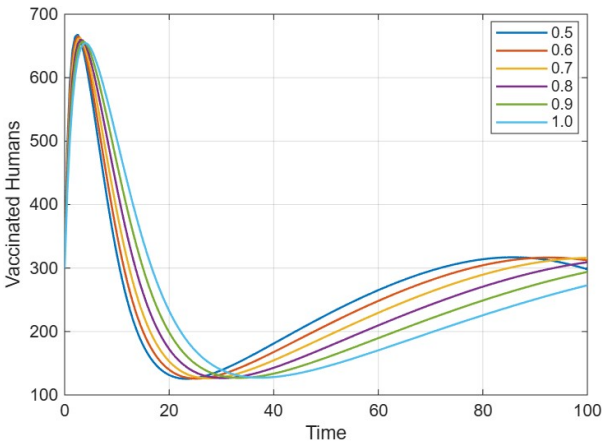

Figure 2. Vaccinated Humans Individuals.

Figure 1 illustrates the behavior of susceptible human individuals over time. An initial sharp decline is observed due to increased exposure to infected individuals during the early stage of

the outbreak.When the control measures and vaccination come in play, the susceptible population slowly stabilizes. The fall and recovery processes are slower with smaller values of the fractional order, which emphasizes the influence of memory in slowing the spread of the disease.

In Figure 2, the population of humans which has been vaccinated is shown. The findings indicate that the rates are high at the start indicating intensive vaccine initiatives. Having reached a peak, the population gradually declines with the help of the waning of the vaccine and natural mortality and comes to the steady state. These transitions are smoothed by the fractional-order effects and postponed the peak value of vaccination.

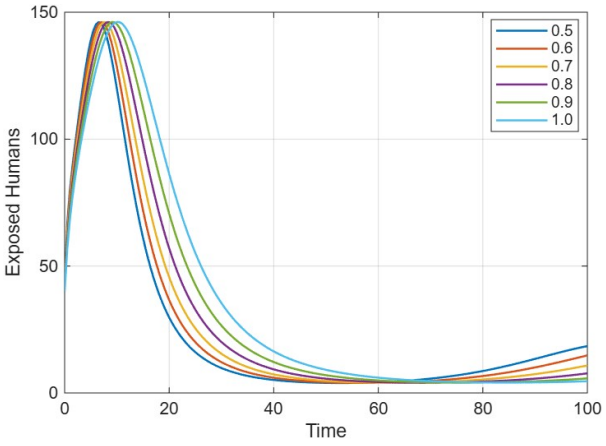

FIGURE 3. Exposed Humans Individuals.

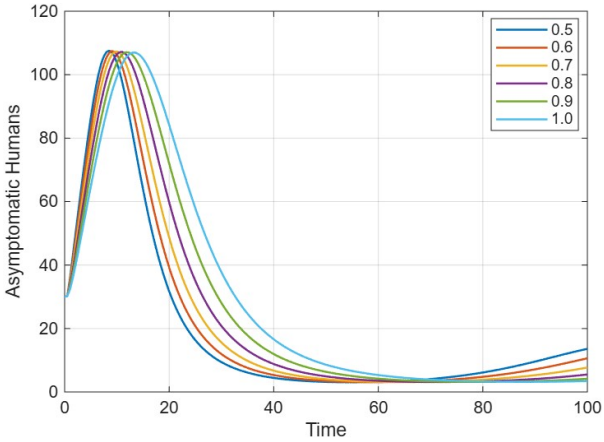

FIGURE 4. Asymptomatic Humans Individuals.

The exposed human population is shown in figure 3. There is a sharp spike during the initial stages, which represents the concentration of the persons in the latent stage of the infection. This population reduces with the course of time as a result of its transition towards asymptomatic and symptomatic categories, which is bolstered by quick testing and isolation measures. The asymptomatic human beings are depicted in figure 4. The figure shows that the number swelled sharply and then gradually dropped, implying that the exposed individuals are first swollen into the category of asymptomatic and subsequently recovered or advanced to symptomatic infection. Reduced fractional orders postpone the peak, which underscores the non-local dynamics of the disease.

The figure 5 depicts the infected (symptomatic) human population. When ideal control measures are used, the peak infection levels significantly reduce. In addition to that, fractional-order dynamics smooth and postpones the peak of an infection, which is epidemiologically significant because it allows to relieve the load on healthcare systems. The treated human population is shown in figure 6. The treated group rises with the identification and medical care being received by the symptomatic people. The number of people decreases with time as a result of recovery and death caused by the disease. Fractional effects help in the seamless treatment dynamics throughout the period of simulation.

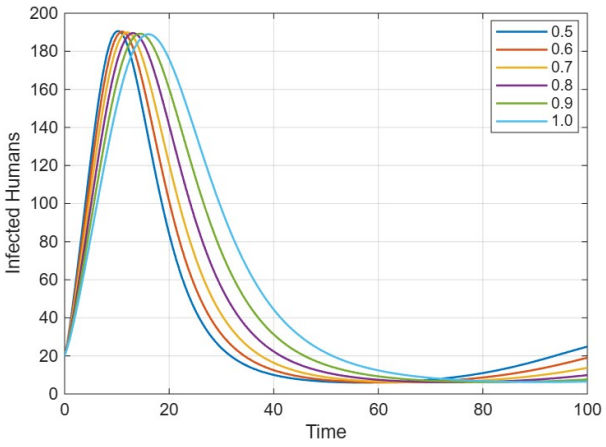

FIGURE 5. Infected Humans Individuals.

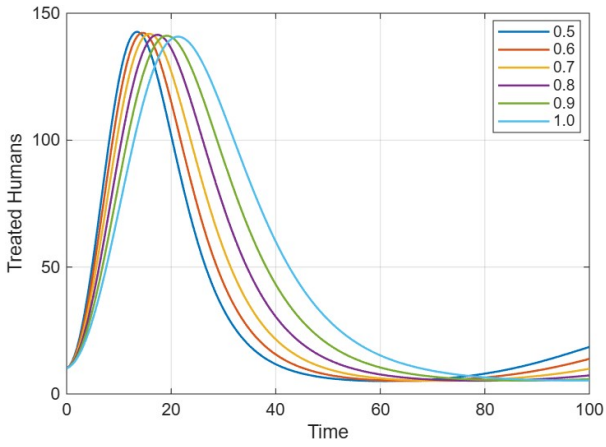

FIGURE 6. Treated Humans Individuals.

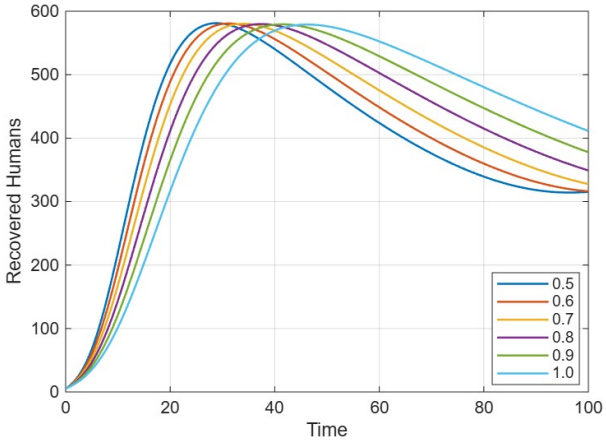

FIGURE 7. Recovery Humans Individuals.

The recovered human population is expressed in figure 7. As the number of both the asymptomatic and treated recovers, there is a gradual rise. At some point, the curves begin to reach a saturation point, which implies that, in the long run, immunity is built up by the population.

The vulnerable population of animals is demonstrated in figure 8. There is rapid early reduction as a result of the spread of infection in the animal reservoir. When the number of infected animals decreases, the susceptible population remains constant and is an indication of less transmission pressure. The exposed animal individuals are shown in figure 9. Just like human case, there is sharp early peak, and then it becomes decreasing as animals transition to the infected or recovered classes.

The population of the infected animals is shown in figure 10. The findings show that the peak of infection is early and then falls very fast because of recovery and deaths caused by the disease. The delay of the peak and prolongation of the period of infection are realized by the fractional-order dynamics.

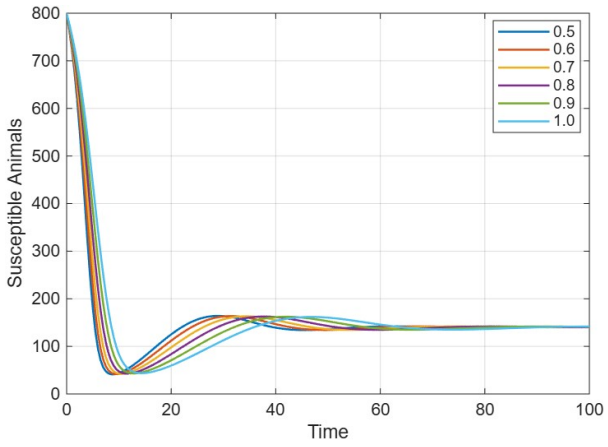

FIGURE 8. Susceptible Animal Individuals.

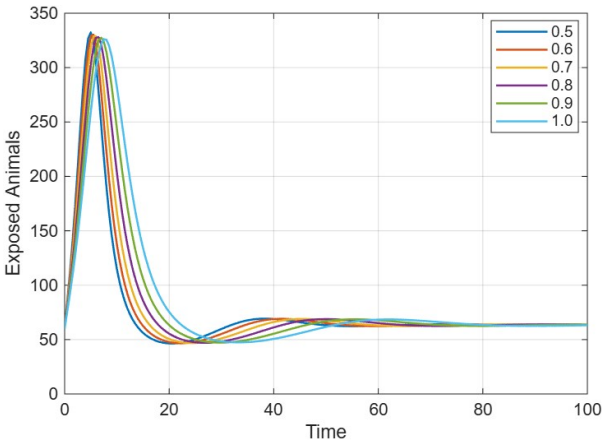

FIGURE 9. Exposed Animal Individuals.

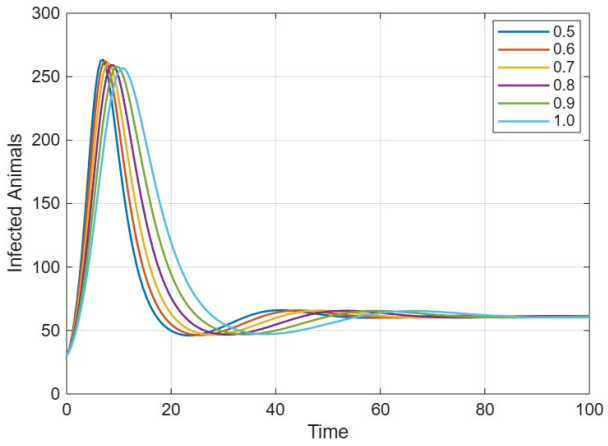

FIGURE 10. Infected Animal Individuals.

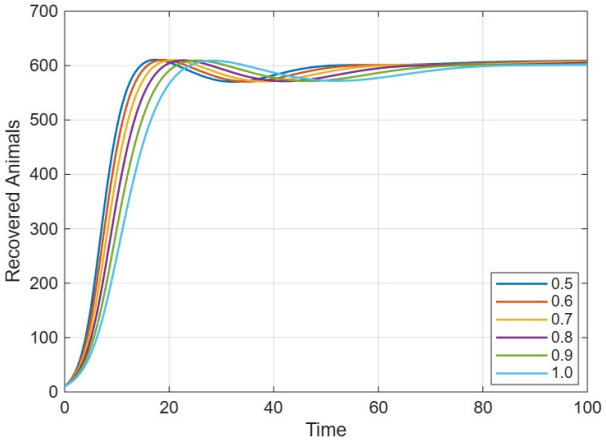

FIGURE 11. Recovery Animal Individuals.

The recovered population of the animals is illustrated in Figure 11. This is observed to be growing steadily as the infected animals recover to a steady point, which implies that immunity in the animal reservoir would last long.

The optimal prevention and isolation control is given in figure 12 as u_1. The intensity of control reaches its peak at the onset of the outbreak with the objective of lowering the rates of effective contacts. With the decline of the epidemic, the control reduces slowly. The figure below, 13, shows the optimal vaccination control, u_2. Immunization activities are high at the initial stage to combat the spread of the disease and reduce as the population level immunity is attained. immunity is achieved.

Figure 14 illustrates the optimal rapid testing control u_3. The control is high at the beginning due to the significance of early detection of people who are exposed to the virus and declines in proportion with a reduction in infections. The optimal treatment control is indicated in Figure 15, u_4. The highest intensity of treatment occurs in the peak infection period and then it decreases slowly as the number of people with infections decreases.

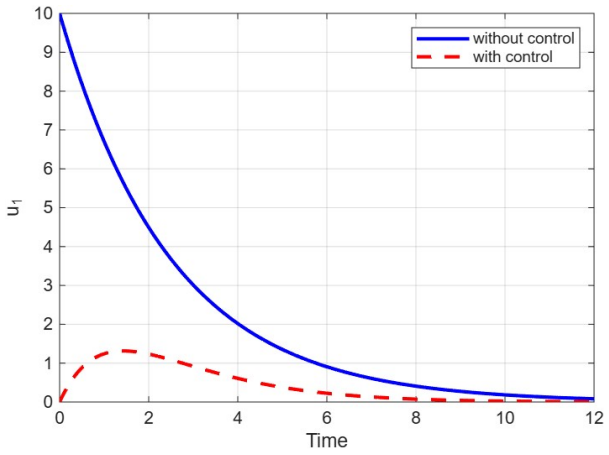

FIGURE 12. u_1 Optimal Control Individuals.

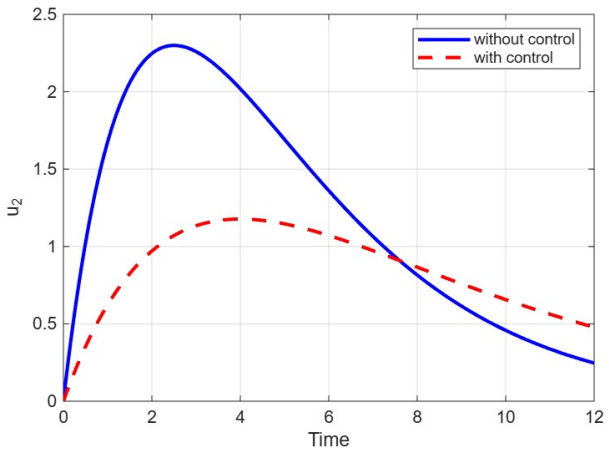

FIGURE 13. u_2 Optimal Control Individuals.

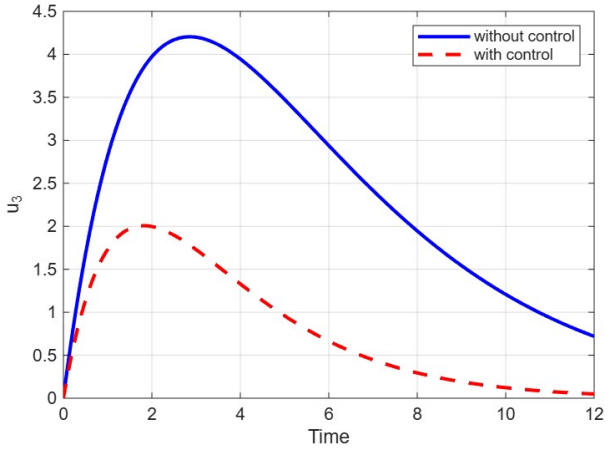

FIGURE 14. u_3 Optimal Control Individuals.

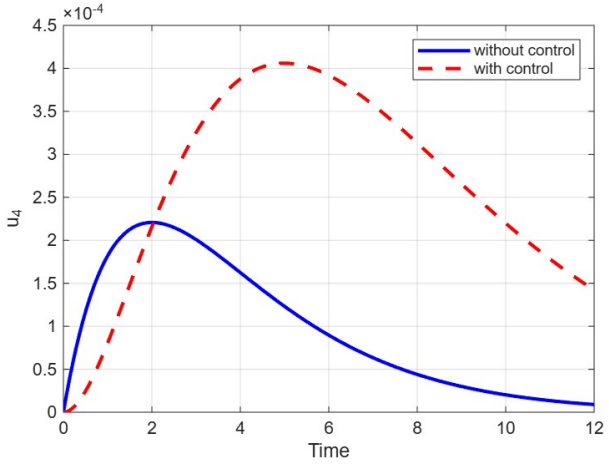

FIGURE 15. u_4 Optimal Control Individuals.

The graphical findings suggest that social distancing, mask-wearing, hand sanitization, vaccination, rapid testing and early treatment are important controls that can be used to mitigate the Monkeypox virus infection in the community. The use of these controls results in quicker reduction in infection cases, which could reduce the strain on the population and economy. Given the huge losses made by the Monkeypox virus, governments need to implement standard operating procedures (SOPs) and limit people to risky areas. Governments should enforce regulations that protect people such as avoiding places that expose them to risk, and it is essential to deal with Monkeypox. With vaccinations and precaution, we will be able to cushion our communities and economies against such damages as diseases such as Monkeypox cause.

In general, these quantitative findings support the idea that the integration of the fractional-order modeling with the optimal control strategies is a powerful tool that can help to reduce the level of infection, postpone the outbreak, and enhance the effectiveness of disease management. The classical integer-order models are more realistic than the fractional framework because they

do not model memory and persistence effects on epidemics, which are inherent in monkeypox transmission.

7. AI-Based Application Using Physics-Informed Neural Networks

This part of the study describes the incorporation of AI methods into the studied ABC-fractional monkeypox transmission model through the use of *Physics-Informed Neural Networks* (PINNs). The purpose here is to create a computational framework that is physics-consistent and at the same time data-driven. This framework will be able to approximate the solution of the ABC-fractional system (3.2), will understand the fractional order's role in memory by its effect on the learning and will finally, give more comprehensive predictions even with little epidemiological data available.

7.1. **Motivation for Using PINNs.**

Non-local operators, such as the Atangana–Baleanu–Caputo (ABC) fractional derivative, make it possible to use fractional-order epidemic models that can realistically represent the memory and hereditary effects that are inherit in the transmission of diseases. On the other hand, classical integer-order models do not have this possibility; they do not allow the present disease dynamics to depend on past states. This is especially important for monkeypox because of the long incubation and infectious periods, and that immunity may well have waned by then. In spite of their great modeling advantages, ABC-fractional models are usually difficult to analyze and expensive to compute, mainly because the fractional derivative adds non-locality in time.

In real life, monkeypox surveillance data is generally scant, unsorted and sometimes totally or partly missed or reported late. These problems limit the application of numerical methods that are traditional, which most of the time demand dense and high-quality data and fine temporal discretization in order to be stable and accurate. Therefore, it is the case that the demand arises for computational techniques that would be able to manage the restricted data with effectiveness while still being in tune with the basic epidemiological mechanisms.

The Physics-Informed Neural Networks (PINNs), which were first introduced by Raissi et al. [21], provide a ground and flexible system that links mechanistic modeling and data-driven learning. The PINNs do so by incorporating the differential equations that govern the system in the training process of neural networks through the use of physics-based loss functions. Thus, it is made sure that the solutions learned are not just data-driven but are also limited to the dynamics of the epidemic according to the ABC-fractional monkeypox model.

Along with that, another benefit of using PINNs is that they do not time-discretize the fractional operator, which means that the solution can be viewed as a smooth and continuous function of time. This characteristic can be said to be most advantageous in the case of fractional-order systems where non-locality can make the computation very complex and costly. In addition, PINNs provide a natural way to do parameter estimation and uncertainty quantification since they treat the parameters of the model that are unknown and the fractional order as variables that can be trained.

Thus, combining the ABC-fractional monkeypox model with PINNs gives an active and trustworthy computational device for the approximation of system dynamics, learning of memory effects, and enhancement of predictive ability in the case of data limitations. The partnership between fractional calculus and AI boosts the usability of the model for both near real-time epidemic analysis and public health decision making.

7.2. **Neural Network Architecture.** Let's denote the state vector of the monkeypox transmission model by

$$\mathbf{U}(\varpi) = \Big(S_H, V_H, E_H, A_H, I_H, T_H, R_H, S_A, E_A, I_A, R_A\Big)$$

where every component shows the temporal change of the related epidemiological compartment in both the human and animal populations.

To solve the ABC-fractional system (3.2), a fully connected feedforward neural network is used for its approximation. The network is structured in such a way to learn a nonlinear mapping from the time domain to the epidemiological state space, which is represented as follows:

$$\widehat{\mathbf{U}}(\varpi;\Theta) \approx \mathbf{U}(\varpi),$$

In this equation, $\widehat{\mathbf{U}}$ is the neural network approximation, and Θ is the set of trainable parameters, which includes weights and biases in all layers.

Words of time variable $\varpi\,\varpi$ enter the network single-handedly, while the output layer is made up of eleven neurons that depict the eleven compartments of the model. This multi-output formulation allows the network to internalize the intrinsic coupling of different epidemiological states and guarantees a synchronized approximation of full system dynamics. To ensure smooth activation functions for neural network output, which is important for identifying fractional derivatives and enforcing the governing equations during training, differentiability is used.

7.3. **PINN Formulation for the ABC-Fractional Model.** Incorporating the epidemiological structure of the ABC-fractional monkeypox model into the learning process, physics-informed residual functions are defined for each equation in system (3.2). These residuals quantify the error between the neural network predictions and the governing ABC-fractional dynamics at the collocation points in the temporal domain selected.

For example, the residual for the susceptible human population is provided as

$$\mathcal{R}_{S_H}(\varpi) = {}_0^{ABC}D_{\varpi}^{\alpha}(\widehat{S_H}) - \Big[\Lambda_h - \lambda_H\widehat{S_H} + \omega\widehat{V_H} - (v+\mu_h)\widehat{S_H}\Big],$$

where ${}_0^{ABC}D_{\varpi}^{\alpha}(\cdot)$ represents the Atangana–Baleanu–Caputo fractional derivative of order α, and the terms on the right-hand side express the epidemiological mechanisms responsible for recruitment, infection, vaccination, and natural mortality.

The same technique was used to create the residual functions for all remaining compartments in the human and animal populations. The role of each residual is to impose its corresponding fractional differential equation through a penalty that is proportional to the extent of the deviation between the neural network approximation and the model dynamics. Therefore, during the

training process, the solution learned becomes a weakly valid solution of the ABC-fractional system over the entire time interval as putting the residuals to the minimum does.

It is through the use of these residuals in the loss function that the PINN framework obliges the neural network to comply with the basic epidemiological principles, thus yielding results that are consistent with the laws of nature, continuous over time, and impervious to being affected by the presence of limited data or noise.

7.4. **Lost Function Construction.** The training of the Physics-Informed Neural Network is being powered by a composite loss function that gives weight to physical consistency, initial condition enforcement, and data fidelity. The total loss function is given by

$$\mathcal{L} = \mathcal{L}_{\text{res}} + \mathcal{L}_{\text{IC}} + \mathcal{L}_{\text{data}}, \tag{7.1}$$

where each part is facilitating the learning process in a particular way.

The loss associated with the residuals, $\mathcal{L}_{\text{res}}$, compels support to the governing equations of the monkeypox model, which are of the ABC-fractional type. It is expressed as

$$\mathcal{L}_{\text{res}} = \frac{1}{N_r} \sum_{i=1}^{N_r} \sum_{k=1}^{11} \left| \mathcal{R}_k(\varpi_i) \right|^2,$$

with $\{\varpi_i\}_{i=1}^{N_r}$ indicating a group of collocation points spread over the temporal domain and $\mathcal{R}_k$ being the physics-informed residual connected to the k-th epidemiological compartment. The loss of this term guarantees that the neural network approximation is weakly in the domain of the ABC-fractional dynamics.

The initial condition loss $\mathcal{L}_{\text{IC}}$ makes sure that there is a strong coherence between the neural network predictions and the initial epidemiological states specified. The loss function is expressed as

$$\mathcal{L}_{\text{IC}} = \sum_{j} \left| \widehat{U}_j(0) - U_{j,0} \right|^2,$$

in which $U_{j,0}$ signifies the starting point of the j-th compartment. This loss function thus fixes the learned solution at time zero and stops it from traveling non-physically far away from the initial state point $\varpi = 0$.

The data mismatch loss $\mathcal{L}_{\text{data}}$ which is the main component of the training, takes into account the available epidemiological observations like reported infected cases, to the training process. When observational data are at hand, this term adds the discrepancies between the network forecasts and the measured values as penalties, thereby enhancing the accuracy of the predictions. If there is no trustworthy data at hand, this term can be ignored, thus allowing the PINN to function solely on a physics-informed basis.

7.5. **Learning the Fractional Order and Model Parameters.** One of the most important strengths of the PINN framework is the fact that it is capable of concurrently approximating state variables and estimating unknown or uncertain model parameters. In the current study, the fractional order

α of the ABC derivative and some chosen epidemiological parameters are considered as trainable variables and optimized during the learning process.

By putting α directly into the loss function, the network is granted the capability of being able to determine the effective memory strength that controls monkeypox transmission from the system dynamics and the data available. This method of implicitly estimating the fractional order by the data provides a very good understanding of the non-local temporal effects that are present in the epidemic process and that cannot be easily quantified using traditional numerical methods.

The simultaneous learning of the state variables and parameters makes the proposed framework more flexible and robust. It opens the door to adaptive model calibration, reduces reliance on parameter assumptions, and consequently enhances the overall predictive capability of the ABC-fractional monkeypox model incorporated with uncertainty.

7.6. **Numerical Results and Discussion.** The proposed Physics-Informed Neural Network's performance is assessed in this subsection by juxtaposing the PINN-based solutions with the numerical solutions of the ABC-fractional monkeypox model for various values of the fractional order $\alpha \in (0, 1]$. The numerical reference solutions are computed by means of the Atangana–Baleanu–Caputo operator that is consistent with a suitable fractional numerical scheme.

A comparison between the PINN approximation and the fractional numerical solution for the infected human population $I_H(\varpi)$ is shown in Figure 16. The PINN framework provides a smooth and continuous approximation without the need for explicit time discretization, and thus accurately captures the nonlinear and memory-driven dynamics of the model. Excellent agreement was obtained between the two methods for the entire time domain.

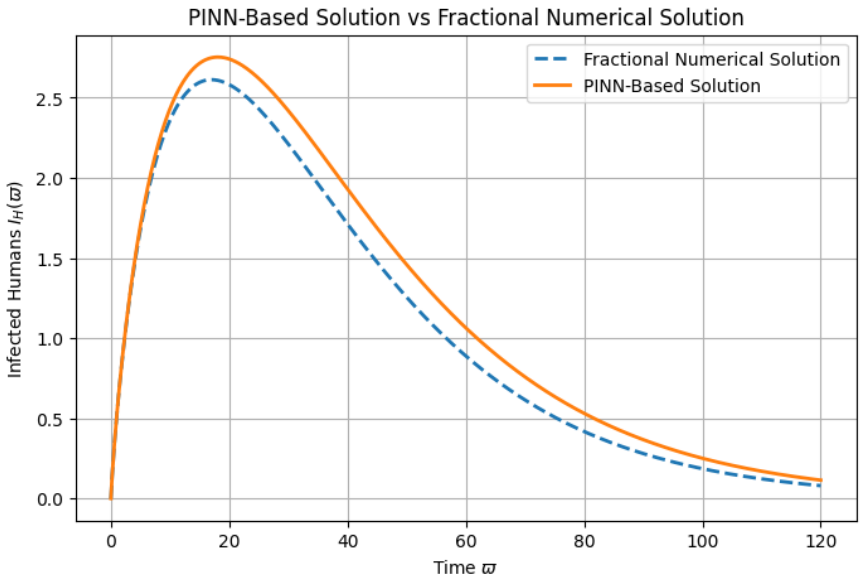

FIGURE 16. Comparison between PINN-based solution and fractional numerical solution for the infected human population $I_H(\varpi)$ under different values of the fractional order α.

Figure 17 depicts the influence of the fractional order α on the dynamics of monkeypox transmission. Reducing the fractional order results in a significant postponement of the epidemic peak and an increase in the time before total eradication of the population. This pattern mirrors the influence of memory and hereditary effects that are introduced via the ABC-fractional derivative and are not accounted for by classical integer-order models.

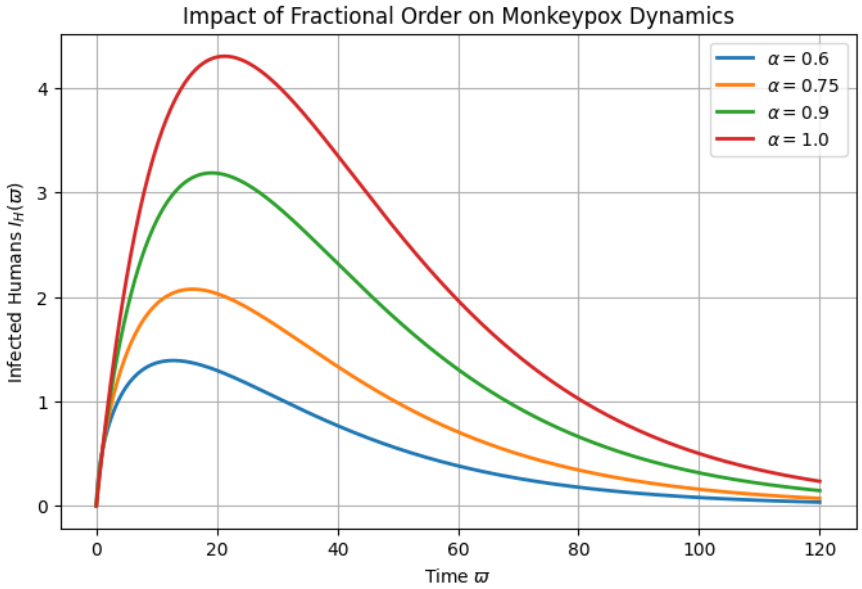

FIGURE 17. Impact of the fractional order α on the dynamics of monkeypox transmission.

Summarizing, the numeral outputs confirm the precision and the cost-effectiveness of the PINN-based method, which thus turns out to be a dependable alternative to the classic fractional numerical solvers, especially in the case of the high-dimensional epidemic models.

7.7. **Implications for Public Health Decision-Making.** The new PINN-assisted ABC-fractional approach is a powerful and speedy analysis and management tool for monkeypox transmission dynamics. By integrating fractional-order modeling with physics-informed machine learning, the new method (a.k.a. "the framework") is able to realize and represent the non-local memory effects that are common in infectious disease spread and the real-time adaptability that comes from the neural network learning. This combination empowers perfect scenario simulation even with very sparse, noisy, or incomplete epidemiological data which is usually the case with the new zoonotic diseases.

The framework supports a rapid assessment of the impact of different intervention measures like vaccination, isolation, and treatment campaigns by assessing their impact on infection prevalence and epidemic progression. By using lower fractional orders that represent stronger memory effects, which in turn provide information about the delayed epidemic peaks and the presence of infection for a longer period, policymakers are thus enabled to foresee possible resurgences and

to empower their resource allocation in a more efficient manner. Moreover, the PINN's capability to extract uncertain model parameters from the available data improves the accuracy of forecasts and enables the adoption of scenario planning under different epidemiological settings.

Overall, the method that combines fractional and AI-based techniques results in a strong decision-support solution for the public health authorities. It supports evidence-based prediction, quick discovery of high-risk times, and the fine-tuning of intervention tactics, thus raising preparedness and reaction to monkeypox outbreaks and at the same time aiding the larger purpose of epidemic control and cost-effective disease management.

8. Conclusion

In the current research, we came up with an innovative monkeypox transmission model that employed the Atangana-Baleanu-Caputo (ABC) fractional derivative to represent memory and hereditary effects in the course of the disease. The existence and uniqueness of solutions were guaranteed through fixed-point theory, which was applied to prove the well-posedness of the fractional-order system. The treatment of an optimal control problem was to reduce infection levels associated with costs of treatment and preventive measures through a trade-off. Under the Maximum Principle of Pontryagin, the conditions needed for the optimality were derived. A Physics-Informed Neural Network (PINN) framework was used to approximate the solution of the ABC-fractional system, and to extract key epidemiological parameters directly from the governing dynamics as a part of data-driven analysis and enhancing computational efficiency. The numerical simulations showed that while PPIN-based solutions provided a smooth and continuous approximation of the epidemic trajectory, they were also very close to the fractional numerical results. The impact of fractional-order effects was revealed by the results, where it was demonstrated that lower fractional orders caused epidemic peaks to be shifted over a longer time frame and thus, lengthened the period of infection, thereby pointing out the significance of memory in the dynamics of transmission.

Fractional modeling and AI based learning give rise to a computational tool that can be flexible and reliable in real time forecasting of outbreaks, analysis of various situations, and assessment of intervention strategies. It is possible to use it to promote the use of evidence-based public health decision-making since it allows identifying the optimal time to intervene and allocating resources better. Further extensions of this approach to spatial heterogeneity, stochastic effects, and adaptive control strategies are possible in future work to increase the predictive power, as well as to additional emerging infectious diseases.

Funding: This research was supported by the University of Phayao and the Thailand Science Research and Innovation Fund (Fundamental Fund 2026, Grant No. 2268/2568).

Conflicts of Interest: The authors declare that there are no conflicts of interest regarding the publication of this paper.

References

[1] I. Arita, D.A. Henderson, Smallpox and Monkeypox in Non-Human Primates, Bull. World Health Organ. 39 (1968), 277–283. https://pmc.ncbi.nlm.nih.gov/articles/PMC2554549.

[2] A. Atangana, D. Baleanu, New Fractional Derivatives with Nonlocal and Non-Singular Kernel: Theory and Application to Heat Transfer Model, arXiv:1602.03408, 2016. https://doi.org/10.48550/arXiv.1602.03408.

[3] C.P. Bhunu, S. Mushayabasa, Modelling the Transmission Dynamics of Pox-Like Infections, IAENG Int. J. Appl. Math. 41 (2011), 141–149.

[4] S. Chowdhury, M. Forkan, S.F. Ahmed, P. Agarwal, A. Shawkat Ali, et al., Modeling the SARS-Cov-2 Parallel Transmission Dynamics: Asymptomatic and Symptomatic Pathways, Comput. Biol. Med. 143 (2022), 105264. https://doi.org/10.1016/j.compbiomed.2022.105264.

[5] L. Cesari, Optimization–Theory and Applications: Problems with Ordinary Differential Equations, Springer, 1983. https://doi.org/10.1007/978-1-4613-8165-5.

[6] P. Emeka, M. Ounorah, F. Eguda, B. Babangida, Mathematical Model for Monkeypox Virus Transmission Dynamics, Epidemiology: Open Access 8 (2018), 3. https://doi.org/10.4172/2161-1165.1000348.

[7] T. Gunasekar, S. Manikandan, V. Govindan, P. D, J. Ahmad, et al., Symmetry Analyses of Epidemiological Model for Monkeypox Virus with Atangana–Baleanu Fractional Derivative, Symmetry 15 (2023), 1605. https://doi.org/10.3390/sym15081605.

[8] D.L. Heymann, M. Szczeniowski, K. Esteves, Re-Emergence of Monkeypox in Africa: A Review of the Past Six Years, Br. Med. Bull. 54 (1998), 693–702. https://doi.org/10.1093/oxfordjournals.bmb.a011720.

[9] A.H. Fan, Topological Wiener-Wintner Ergodic Theorem with Polynomial Weights, Chaos, Solitons Fractals 117 (2018), 105–116. https://doi.org/10.1016/j.chaos.2018.10.015.

[10] W.O. Kermack, A.G. McKendrick, A Contribution to the Mathematical Theory of Epidemics, Proc. R. Soc. Lond. Ser. A 115 (1927), 700–721. https://doi.org/10.1098/rspa.1927.0118.

[11] A. Kumar, P.K. Srivastava, Y. Dong, Y. Takeuchi, Optimal Control of Infectious Disease: Information-Induced Vaccination and Limited Treatment, Physica A: Stat. Mech. Appl. 542 (2020), 123196. https://doi.org/10.1016/j.physa.2019.123196.

[12] I.D. Ladnyj, P. Ziegler, E. Kima, A Human Infection Caused by Monkeypox Virus in Basankusu Territory, Democratic Republic of the Congo, Bull. World Health Organ. 46 (1972), 593–597. https://pmc.ncbi.nlm.nih.gov/articles/PMC2480792.

[13] A. Momoh, M. Ibrahim, I. Uwanta, S. Manga, MATHEMATICAL MODEL FOR CONTROL OF MEASLES EPIDEMIOLOGY, Int. J. Pure Apllied Math. 87 (2013), 707–718. https://doi.org/10.12732/ijpam.v87i5.4.

[14] O.J. Peter, F.A. Oguntolu, M.M. Ojo, A. Olayinka Oyeniyi, R. Jan, et al., Fractional Order Mathematical Model of Monkeypox Transmission Dynamics, Phys. Scr. 97 (2022), 084005. https://doi.org/10.1088/1402-4896/ac7ebc.

[15] O.J. Peter, C.E. Madubueze, M.M. Ojo, F.A. Oguntolu, T.A. Ayoola, Modeling and Optimal Control of Monkeypox with Cost-Effective Strategies, Model. Earth Syst. Environ. 9 (2022), 1989–2007. https://doi.org/10.1007/s40808-022-01607-z.

[16] L.S. Pontryagin, Mathematical Theory of Optimal Processes, CRC Press, 1987.

[17] M.A. Qurashi, S. Rashid, A.M. Alshehri, F. Jarad, F. Safdar, New Numerical Dynamics of the Fractional Monkeypox Virus Model Transmission Pertaining to Nonsingular Kernels, Math. Biosci. Eng. 20 (2022), 402–436. https://doi.org/10.3934/mbe.2023019.

[18] S. Somma, N. Akinwande, U. Chado, A Mathematical Model of Monkey Pox Virus Transmission Dynamics, Ife J. Sci. 21 (2019), 195–204. https://doi.org/10.4314/ijs.v21i1.17.

[19] S. Usman, I. Isa Adamu, Modeling the Transmission Dynamics of the Monkeypox Virus Infection with Treatment and Vaccination Interventions, J. Appl. Math. Phys. 05 (2017), 2335–2353. https://doi.org/10.4236/jamp.2017.512191.

[20] World Health Organization, Mpox. https://www.who.int/news-room/fact-sheets/detail/mpox.

[21] M. Raissi, P. Perdikaris, G. Karniadakis, Physics-Informed Neural Networks: A Deep Learning Framework for Solving Forward and Inverse Problems Involving Nonlinear Partial Differential Equations, J. Comput. Phys. 378 (2019), 686–707. https://doi.org/10.1016/j.jcp.2018.10.045.

[22] G.E. Karniadakis, I.G. Kevrekidis, L. Lu, P. Perdikaris, S. Wang, et al., Physics-Informed Machine Learning, Nat. Rev. Phys. 3 (2021), 422–440. https://doi.org/10.1038/s42254-021-00314-5.